Local polaron effects in mixed-valence systems: Exact model calculation in the limit of large degeneracy

K. Schönhammer
I. Institut für Theoretische Physik, Universität Hamburg, D-2000 Hamburg 36, Federal Republic of Germany

O. Gunnarsson
Max-Planck-Institut für Festkörperforschung, D-7000 Stuttgart 80, Federal Republic of Germany
(Received 10 February 1984)

The Anderson impurity model including a linear coupling to a local boson mode is solved exactly in the large-degeneracy limit for infinitely large f-f Coulomb repulsion. Ground-state properties and the f-level Green's function are discussed. For a small boson frequency ω_0, two different types of mixed-valence behavior occur, depending on the strength v of the electron-phonon coupling. In the weak-coupling limit the "lattice" shows small fluctuations around its average position, while for a strong-coupling v there exists a narrow regime of energies, ϵ_f, of the f-level where mixed-valence behavior with large mean-square "lattice" deviations occurs. For finite phonon frequencies ω_0, quantum fluctuations smooth out the first-order transition occurring in the limit $\omega_0 \to 0$. In the weak-coupling limit, the mean-field approximation of the electron-phonon coupling, leading to a renormalization of the f-level position, provides a good description of the ground-state properties and the f-level spectrum. In the strong-coupling mixed-valence regime, some ground-state properties can be interpreted in terms of a renormalized f-electron—conduction-electron coupling $\tilde{\Delta} \to \tilde{\Delta} \exp(-v/\omega_0) \equiv \bar{\Delta}$. This renormalization does *not* occur for the width of f-level peak in the one-particle Green's function. In this regime, the f-level spectral function can be described as a superposition of two spectra. The relative weight of these two spectra varies rapidly when ϵ_f varies of the order $\bar{\Delta}$ in the transition regime, while the individual spectra change little. The large-boson-frequency limit ("plasmon case") is also discussed with special emphasis on the renormalization occurring in this limit.

I. INTRODUCTION

The strong correlation between the f electrons in mixed-valence systems[1,2] is responsible for the fact that the electronic properties of these systems cannot properly be described in the one-particle model. Theoretical progress has therefore come mainly from the study of model Hamiltonians such as the Anderson impurity model or the Anderson lattice.[3] An important progress in the treatment of the Anderson model was the realization by Ramakrishnan[4] and Anderson[4] that for the calculation of thermodynamic properties there is a small parameter $1/N_f$, where N_f is the degeneracy of the f level. We have used similar ideas in the calculation of spectral functions[5,6] related to various electron spectroscopies and have presented some exact results in the limit $N_f \to \infty$. We have applied this theory to Ce compounds and, by comparison with experimental data, we have obtained estimates for the f-level occupancy n_f and the coupling Δ of the f level to the conduction states.[6,7] Recently, several other authors have proposed methods for obtaining systematic corrections in $1/N_f$.[8] Using the Bethe-*Ansatz* technique some exact results also have been obtained for finite N_f for the case of an infinitely broad valence band with a constant density of states.[9] As the coupling Δ has usually been assumed to be comparable to the relevant phonon frequencies, and because there is a large difference in the ionic radii associated with the two valence states, the question of strong f-electron—lattice coupling has been considered by various authors.[10–14] All these studies use Anderson-type Hamiltonians coupled linearly to boson mode(s). Similar models have been used in the description of chemisorption on metal surfaces, where the boson is usually considered to be a surface plasmon.[15–17] A formally rather similar problem is the vibration-induced narrowing of electron scattering resonances near threshold.[18] Sherrington and von Molnar[10] concluded that, for low-temperature properties there is a large polaronic reduction of the f-level—conduction-electron coupling, $\Delta \to \Delta \exp(-v/\omega_0)$, if the electron-phonon coupling λ is sufficiently large that the "relaxation energy" $v = \lambda^2/\omega_0$ is much larger than Δ and ω_0. This result is obtained using perturbation theory in the f-level—conduction-electron coupling. Hewson and Newns[12] presented the exact (numerical) solution to the impurity-type model with coupling to one boson mode and with a *single electron* in the system. In a later paper, Hewson and Newns removed the restriction to a single electron and proposed variational *Ansätze* to describe the many-electron system. Concerning the renormalization of Δ, they found[13] more restrictive conditions than Sherrington and von Molnar.[10] A very detailed discussion of phase diagrams for these types of models was given by Haldane, where *both* the f-f Coulomb repulsion and the electron-phonon coupling are treated in a mean-field approximation. The strong correlation between the f elec-

trons and the large degeneracy N_f has been taken into account in a variational *Ansatz* proposed by Kohn *et al.*[14]

In this paper we show that the exact solution to the impurity model with a linear coupling to one boson mode can be obtained in the *large-degeneracy* ($N_f \to \infty$, $N_f \Delta \equiv \tilde{\Delta} = \text{const}$) limit for infinitely large f-f Coulomb repulsion. In Sec. II we introduce the model and reduce the exact ground-state calculation to a pure-boson problem in Sec. III. The exact result for the part of the f-level Green's function that describes valence photoemission is presented in Sec. IV. To obtain explicit results for the ground-state properties and the f level, Green's-function tridiagonal matrices have to be inverted numerically. In Sec. V the limit of a small boson frequency, called the "phonon case," is discussed. To obtain a better understanding of the exact numerical results the (Born-Huang[19]) adiabatic approximation is used to obtain approximate analytical results for the ground state and the spectrum. Phase diagrams of the f-level occupancy in the (ϵ_f, v) plane are presented, where ϵ_f is the (bare) f-level energy. In the limit $\omega_0 \to 0$ the adiabatic theory produces the exact result: At a critical point $(v_{\text{crit}}, (\epsilon_f)_{\text{crit}})$ with $v_{\text{crit}} \sim \tilde{\Delta}$, a critical line $v_c(\epsilon_f) \sim \epsilon_f$ starts, across which there is a first-order transition from n_f occupancies close to 1 to values close to 0. For finite frequencies ω_0, quantum fluctuations smooth out this discontinuous transition. For $v \gg v_{\text{crit}}$ the transition then occurs on an energy scale $\tilde{\Delta} \exp(-v/\omega_0)$, in agreement with the conclusion by Sherrington and von Molnar.[10] *This renormalization does not occur in the width of the effective f level in the f-level Green's function.* The effective f-level position stays close to $\epsilon \approx -v$, i.e., far below the Fermi energy (on the scale of $\tilde{\Delta}$), during the transition, and only the overall weight of the spectrum is reduced. In the narrow mixed-valence regime near $v_c(\epsilon_f)$ the spectrum can be described as a *superposition of two spectra.* Both spectra are *"insensitive"* to changes of ϵ_f by an energy of the order $\tilde{\Delta} \exp(-v/\omega_0)$, while the relative weight factors change very rapidly with ϵ_f. These results show quite clearly that the question of the renormalization of $\tilde{\Delta}$ depends strongly on the property studied.

The mixed-valence behavior for $v < v_{\text{crit}}$ and $v > v_{\text{crit}}$ is very different. For $v < v_{\text{crit}}$ the "lattice" is in an intermediate position with fluctuations that are small compared to the extremes corresponding to the two pure ionic configurations, while for $v > v_{\text{crit}}$ there are fluctuations comparable to the difference in the pure ionic radii. In Sec. VI we discuss the limit of large boson frequency ω_0, called the "plasmon" case. In agreement with conclusions by Hewson and Newns[12,13] for the single-electron case, we find that the question of the renormalization of $\tilde{\Delta}$ depends strongly on the ratio ω_0/B where B is the conduction-band width. In Secs. VII and VIII, a short discussion of the cases $1-n_f \ll 1$ and $n_f \ll 1$ are given. In Sec. IX we summarize our results and discuss what are "realistic" parameters. In two appendixes some of the details of the calculations are given for the limits $B \to 0$ and ∞.

II. MODEL

As discussed in the Introduction, we treat the (single-impurity) Anderson model[3] with an additional coupling to a local boson mode. We use the partial-wave representation for the conduction electrons and introduce a combined index $\nu = (m, \sigma)$ for the orbital and spin degeneracy ($\nu = 1, \ldots, N_f$), which are equivalent in our model,[6]

$$H = \sum_{k,\nu} \epsilon_k n_{k\nu} + \sum_{\nu} \epsilon_f n_\nu + \sum_{k,\nu} V_k (\psi^\dagger_{k\nu} \psi_\nu + \text{H.c.}) + U \sum_{\mu < \nu} n_\mu n_\nu + \omega_0 b^\dagger b + \lambda (b + b^\dagger) \sum_\nu n_\nu \, . \quad (2.1)$$

Here, $\psi^\dagger_{k\nu}$ denotes the creation operator of a conduction electron with the wave number k, and $\psi^\dagger_\nu$ that of an f electron. The hopping between the f level and the conduction states is described by V_k and the Coulomb interaction between the f electrons is given by U. The energy ϵ_f of the f level obtains an additional ν dependence if an external magnetic field is introduced or if one wants to simulate spin-orbit splitting. The operator $b^\dagger$ creates a local phonon mode with the frequency ω_0. The last term in the Hamiltonian (2.1) presents a linear coupling of the oscillator to the total occupancy of the f level. Similar model Hamiltonians have been used previously in the discussion of local polaron effects in mixed-valence system.[10-14] The Hamiltonian (2.1) conserves the number of electrons corresponding to a given value of ν,

$$\left[\psi^\dagger_\nu \psi_\nu + \sum_k \psi^\dagger_{k\nu} \psi_{k\nu}, \, H \right] = 0 \, . \quad (2.2)$$

In the following we will discuss the limit when the degeneracy N_f of the f level goes to infinity. To obtain a proper limit for various physical quantities, the coupling between the f level and the conduction electrons has to be of the form $V_k = \tilde{V}_k / (N_f)^{1/2}$ with $\tilde{V}_k$ independent of N_f. In the limit $U \to \infty$, i.e., when double and higher occupancy of the f level is suppressed, it is possible to construct the exact ground state for $N_f = \infty$.

III. GROUND STATE: GENERAL RESULTS

In the Schrödinger equation for the ground state we split the Hamiltonian (2.1) into three parts,

$$(H_{\text{el}} + H_B^0 + H_{\text{el-}B}) \, | E_0 \rangle = E_0 \, | E_0 \rangle \, , \quad (3.1)$$

an electronic part, the free-boson part, and the electron-boson interaction. The ground state $| E_0 \rangle$ is a state in product space, $\mathscr{H}_{\text{el}} \otimes \mathscr{H}_B$. We now introduce an orthonormal set $| i \rangle$ of the electronic states which are complete in $\mathscr{H}_{\text{el}}$. Then (3.1) can be written as

$$\sum_j [\langle i | H_{\text{el}} | j \rangle + H_B^0 \delta_{ij} + \lambda (b + b^\dagger) \langle i | \hat{n}_f | j \rangle] \, | B_j \rangle = E_0 \, | B_i \rangle \, , \quad (3.2)$$

where the $| B_i \rangle = \langle i | E_0 \rangle$ are boson states and $\hat{n}_f = \sum_\nu \psi^\dagger_\nu \psi_\nu$ is the number operator for the f electrons. In the following we choose basis states $| i \rangle$ which are eigenstates of $\hat{n}_f$. Then (3.2) simplifies to

$$\sum_j [\langle i | H_{\text{el}} | j \rangle + H_B(n_i) \delta_{ij}] \, | B_j \rangle = E_0 \, | B_i \rangle \, , \quad (3.3)$$

with

$$H_B(n_i)=\omega_0 b^\dagger b+\lambda n_i(b+b^\dagger)\ , \tag{3.4}$$

where $n_i=\langle i\,|\,\hat{n}_f\,|\,i\rangle$ is a c-number (0 to 1). The coupling between the $|B_j\rangle$ then is only due to the electronic off-diagonal elements $\langle i\,|\,H_{\rm el}\,|\,j\rangle$. The construction of the electronic basis set now proceeds in complete analogy to the case without the boson mode, which we have presented earlier.[5,6] We first introduce a state

$$|0\rangle=\left[\prod_{\nu=1}^{N_f}\prod_{k\le k_F}\psi^\dagger_{k\nu}\right]|\,\text{vac}\rangle\ , \tag{3.5}$$

where all conduction states below the Fermi energy are occupied and the f level is empty. This state couples via $H_{\rm el}$ to states

$$|\,k\rangle=\frac{1}{(N_f)^{1/2}}\left[\sum_\nu \psi^\dagger_\nu\psi_{k\nu}\right]|0\rangle\ , \tag{3.6}$$

with one f electron and one hole below the Fermi energy. For $U=\infty$, these states only couple (apart from coupling to $|0\rangle$) to further states,

$$|\,\kappa,k\rangle=\frac{1}{(N_f)^{1/2}}\left[\sum_\nu \psi^\dagger_{\kappa\nu}\psi_{k\nu}\right]|0\rangle\ , \tag{3.7}$$

with one electron above the Fermi energy ($\kappa>k_F$) and one hole ($k\le k_F$). The matrix elements of $H_{\rm el}$ with these basis states are given by

$$\langle 0\,|\,H_{\rm el}\,|\,0\rangle=E_0^0\ , \tag{3.8}$$

$$\langle k\,|\,H_{\rm el}\,|\,k'\rangle=\delta_{kk'}(E_0^0-\epsilon_k+\epsilon_f)\ , \tag{3.9}$$

$$\langle 0\,|\,H_{\rm el}\,|\,k\rangle=\tilde{V}_k\ , \tag{3.10}$$

$$\langle k\,|\,H_{\rm el}\,|\,\kappa,k'\rangle=\delta_{kk'}\tilde{V}_\kappa/(N_f)^{1/2}\ , \tag{3.11}$$

$$\langle\kappa,k\,|\,H_{\rm el}\,|\,\kappa',k'\rangle=\delta_{kk'}\delta_{\kappa\kappa'}(E_0-\epsilon_k+\epsilon_\kappa)\ . \tag{3.12}$$

For arbitrary large but finite systems (i.e., a discrete set of ϵ_k), the total Hilbert space of the problem separates into disconnected parts in the limit $N_f\to\infty$ if we choose $V_k=\tilde{V}_k/(N_f)^{1/2}$ with $\tilde{V}_k$ independent of N_f. From Eq. (3.11) we see that the set of states $\{|0\rangle,|\,k\rangle\}$ is disconnected from the rest of the electronic Hilbert space in this limit. The same would happen if instead of starting from $|0\rangle$, we start from an other state which already has electron-hole pairs present. As $|0\rangle$ has the lowest energy to start with, the electronic basis set $\{|0\rangle,|\,k\rangle\}$ leads to the exact ground state in the limit $N_f\to\infty$. With (3.8)—(3.10), Eq. (3.3) then reads

$$[E_0^0+H_B(0)]\,|B_0\rangle+\sum_k\tilde{V}_k\,|B_k\rangle=E_0\,|B_0\rangle\ , \tag{3.13}$$

$$\tilde{V}_k\,|B_0\rangle+[E_0^0+\epsilon_f-\epsilon_k+H_B(1)]\,|B_k\rangle=E_0\,|B_k\rangle\ .$$

After eliminating $|B_k\rangle$, one obtains an eigenvalue equation for $|B_0\rangle$ only,

$$\{H_B(0)-\tilde{\Gamma}[\epsilon_f-\Delta E+H_B(1)]\}\,|B_0\rangle=\Delta E\,|B_0\rangle\ , \tag{3.14}$$

with $\Delta E=E_0-E_0^0$ and

$$\tilde{\Gamma}(z)=\sum_{k\le k_F}\frac{|\,\tilde{V}_k\,|^2}{z-\epsilon_k}\ . \tag{3.15}$$

The ground state is given by

$$|\,E_0\rangle=\left[|0\rangle-\sum_{k\le k_F}\frac{\tilde{V}_k}{\epsilon_f-\Delta E+H_B(1)-\epsilon_k}\,|\,k\rangle\right]|B_0\rangle\ . \tag{3.16}$$

To determine the ground-state-energy shift ΔE one must solve Eq. (3.14). To obtain a more explicit form of this equation, we introduce the eigenstates $|\,\tilde{n}\rangle_B$ of $H_B(1)$,

$$H_B(1)\,|\,\tilde{n}\rangle_B=\left[n\omega_0-\frac{\lambda^2}{\omega_0}\right]|\,\tilde{n}\rangle_B\ . \tag{3.17}$$

Multiplying (3.14) to the left with ${}_B\langle\tilde{n}\,|$ leads to an infinite set of coupled equations for the coefficients $\tilde{b}_n\equiv{}_B\langle\tilde{n}\,|\,B_0\rangle$,

$$\left[n\omega_0+\frac{\lambda^2}{\omega_0}-\Delta E-\tilde{\Gamma}\left[\epsilon_f-\Delta E-\frac{\lambda^2}{\omega_0}-n\omega_0\right]\right]\tilde{b}_n$$
$$-\lambda(\sqrt{n}\,\tilde{b}_{n-1}+\sqrt{n+1}\,\tilde{b}_{n+1})=0\ . \tag{3.18}$$

Owing to the tridiagonal form[12,18] of the matrix coupling the $\tilde{b}_n$, it is possible to solve these equations numerically even if one has to go to very large n before the equations can be truncated. Numerical results will be presented in Secs. V and VI. In the variational *Ansatz* used by Kohn *et al.*,[14] the boson states

$$|\,B_k\rangle=\frac{-\tilde{V}_k}{\epsilon_f-\Delta E+H_B(1)-\epsilon_k}\,|B_0\rangle \tag{3.19}$$

are replaced by $a_k\,|\,A\rangle$, where the a_k are c-numbers and $|\,A\rangle$ is a (variational) boson state *independent* of k. This *Ansatz* therefore leads only to the exact solution in the narrow-band limit $B\to 0$.

To obtain a better understanding of the nature of the ground state, it is useful to calculate expectation values. In particular, we have calculated $\langle E_0\,|\,\hat{n}_f A\,|\,E_0\rangle$ and $\langle E_0\,|\,(1-\hat{n}_f)A\,|\,E_0\rangle$ where A is an arbitrary boson operator. Using (3.16) one obtains

$$\langle E_0\,|\,(1-\hat{n}_f)A\,|\,E_0\rangle=\sum_{m,n}\tilde{b}_m\,{}_B\langle\tilde{m}\,|\,A\,|\,\tilde{n}\rangle_B\,\tilde{b}_n\ , \tag{3.20}$$

$$\langle E_0\,|\,\hat{n}_f A\,|\,E_0\rangle=-\sum_n(\tilde{b}_n)^2\,{}_B\langle\tilde{n}\,|\,A\,|\,\tilde{n}\rangle_B\,\tilde{\Gamma}'(\delta+n\omega_0)$$
$$-\sum_{m\ne n}\tilde{b}_m\,{}_B\langle\tilde{m}\,|\,A\,|\,\tilde{n}\rangle_B\,\tilde{b}_n\times\frac{\tilde{\Gamma}(\delta+n\omega_0)-\tilde{\Gamma}(\delta+m\omega_0)}{(n-m)\omega_0}\ , \tag{3.21}$$

with $\delta=\epsilon_f-\Delta E-\lambda^2/\omega_0$ and $\tilde{\Gamma}'(z)$ the derivative of $\tilde{\Gamma}(z)$ with respect to z. To obtain expectation values of pure-boson operators, one must simply add the two results. The f-level occupancy, n_f is obtained by setting $A=1$ in Eq. (3.21).

The nature of the ground state strongly depends on the coupling strength λ and how the oscillator frequency ω_0 compares to typical electronic energies in the problem. In the limit of "small" ω_0 ("phonon case"), as well as in the limit of very large ω_0 ("plasmon case"), it is possible to obtain approximate analytic solutions to (3.14). It is therefore useful to present the exact numerical results for both limits separately and to compare them with the approximate analytical results. This is done in Secs. V and VI. In the next section we derive the exact result for the part of f-level Green's function which describes photoemission from the f level.

IV. VALENCE PHOTOEMISSION: GENERAL RESULTS

Photoemission from the valence electrons is an important tool for studying electronic properties of mixed-valence systems. We therefore present the exact $N_f\to\infty$ result of the part $g_f^<$ of the f-level Green's function which describes photoemission from the f level,[5,6]

$$g_f^<(z)=N_f\left\langle E_0\left|\psi_\nu^\dagger\frac{1}{z-E_0+H}\psi_\nu\right|E_0\right\rangle . \tag{4.1}$$

With the use of our result for the ground state (3.16), this can be written as

$$g_f^<(z)=\sum_{k,k'}\left\langle B_0\left|\frac{\tilde{V}_k}{\epsilon_f-\Delta E+H_B(1)-\epsilon_k}\langle k,\nu\,|\,G(z)\,|\,k',\nu\rangle\frac{\tilde{V}_{k'}}{\epsilon_f-\Delta E+H_B(1)-\epsilon_{k'}}\right|B_0\right\rangle , \tag{4.2}$$

where the summations are restricted to $k,k'\le k_F$,

$$|\,k,\nu\rangle=\psi_{k\nu}|\,0\rangle , \tag{4.3}$$

and

$$G(z)=(z-E_0+H)^{-1} . \tag{4.4}$$

To evaluate the resolvent matrix element $\langle k,\nu\,|\,G\,|\,k',\nu\rangle$, we start from the identity

$$\langle k,\nu\,|\,(z-E_0+H)G(z)\,|\,k',\nu\rangle=\delta_{kk'} ,$$

and insert those basis states between H and $G(z)$ which in the limit $N_f\to\infty$ couple via H to $|\,k',\nu\rangle$. Analogous to the case without phonon coupling,[5,6] these are the states

$$|\,k,\nu;k'\rangle=\frac{1}{(N_f-1)^{1/2}}\sum_{\nu'(\neq\nu)}\psi_{\nu'}^\dagger\psi_{k'\nu'}\psi_{k\nu}|\,0\rangle . \tag{4.5}$$

The coupling to the states with two holes in the "ν channel" can be neglected in the limit $N_f\to\infty$. The coupling of the states (4.5) to states different from the states (4.3) goes to zero in the limit $N_f\to\infty$. With the matrix elements

$$\begin{aligned}
&\langle k,\nu\,|\,H\,|\,k',\nu\rangle=\delta_{kk'}[E_0^0-\epsilon_k+H_B(0)] ,\\
&\langle k,\nu\,|\,H\,|\,k',\nu;k''\rangle=\delta_{kk'}\left[\frac{N_f-1}{N_f}\right]^{1/2}\tilde{V}_{k''} ,\\
&\langle k,\nu;k'\,|\,H\,|\,k'',\nu;k'''\rangle\\
&\qquad=\delta_{kk''}\delta_{k'k'''}[E_0^0-\epsilon_k-\epsilon_{k'}+\epsilon_f+H_B(1)] ,
\end{aligned} \tag{4.6}$$

this leads to a system of coupled equations

$$\begin{aligned}
&[z-\Delta E-\epsilon_k+H_B(0)]\langle k,\nu\,|\,G\,|\,k',\nu\rangle\\
&\qquad+\sum_{k''}\tilde{V}_{k''}\langle k,\nu;k''\,|\,G\,|\,k'\nu\rangle=\delta_{kk'} ,
\end{aligned} \tag{4.7}$$

$$\begin{aligned}
&[z-\Delta E-\epsilon_k-\epsilon_{k''}+\epsilon_f+H_B(1)]\langle k,\nu;k''\,|\,G\,|\,k',\nu\rangle\\
&\qquad+\tilde{V}_{k''}\langle k,\nu\,|\,G\,|\,k',\nu\rangle=0 .
\end{aligned}$$

Here we have replaced the square root appearing in (4.7) by 1 because we only discuss the limit $N_f\to\infty$. These equations can be easily solved and one obtains

$$\begin{aligned}
&\langle k,\nu\,|\,G(z)\,|\,k',\nu\rangle\\
&\quad=\{z-\Delta E-\epsilon_k+H_B(0)\\
&\qquad-\tilde{\Gamma}[z-\Delta E+\epsilon_f-\epsilon_k+H_B(1)]\}^{-1}\delta_{kk'} .
\end{aligned} \tag{4.8}$$

If this is inserted into (4.2) we have reduced the calculation of $g_f^<(z)$ to a pure-boson problem,

$$\begin{aligned}
g_f^<(z)=\sum_{k\le k_f}|\,\tilde{V}_k\,|^2\langle B_0\,|\,h_k^{-1}[z-h_k-\epsilon_f-\lambda(b+b^\dagger)\\
-\tilde{\Gamma}(z-h_k)]^{-1}h_k^{-1}\,|\,B_0\rangle ,
\end{aligned} \tag{4.9}$$

where we have introduced the abbreviation

$$h_k=\epsilon_k+\Delta E-\epsilon_f-H_B(1) . \tag{4.10}$$

To obtain an expression for $g_f^<(z)$ suitable for the numerical calculation one inserts the complete set of eigenstates of $H_B(1)$, Eq. (3.17), in the matrix element of (4.9). Then one has to invert a tridiagonal matrix for every value of z. In the limit $\lambda\to 0$, $|\,B_0\rangle\to|\,\tilde{0}\rangle_B$, and $g_f^<(z)$ properly reduces to the exact $N_f\to\infty$ result without coupling to the boson presented earlier.[5,6] For the zero-coupling case ($\lambda=0$), there is an exact relation between the spectral function $\rho_f(\epsilon)=\mathrm{Im}[g_f^<(\epsilon-i0]/\pi$ at the Fermi energy ϵ_F and the locally displaced charge, which, for a broad valence band, can be expressed in terms of the f-level occupancy n_f.[20] Below, we generalize this relation to finite electron-boson coupling, λ. This can be done starting directly from the exact ($N_f=\infty$) solution (4.9).

A more transparent procedure is to use the spectral rep-

resentation for $\rho_f(\epsilon)=\mathrm{Im}[g_f^<(\epsilon-i0)]/\pi$,

$$\rho_f(\epsilon)=N_f\sum_{k,\alpha}|\langle E_{k,\nu,\alpha}^{N-1}|\psi_\nu|E_0^N\rangle|^2\delta(\epsilon-(E_0^N-E_{k\nu,\alpha}^{N-1}))\ , \tag{4.11}$$

where the $|E_{k\nu,\alpha}^{N-1}\rangle$ are the exact eigenstates of the system with $N-1$ electrons, which can be constructed in analogy to the procedure for the ground state $|E_0^N\rangle$ described in Sec. III. The only difference is that we have to use the states $|k,\nu\rangle=\psi_{k\nu}|0\rangle$ instead of $|0\rangle$ as the basic electronic state to construct the eigenstates. The lowest state for each of the resulting sets of eigenstates is denoted by $|E_{k\nu,0}^{N-1}\rangle$. Apart from correction terms which vanish in the limit $N_f\to\infty$, $|E_{k\nu,0}^{N-1}\rangle\to\psi_{k\nu}|E_0^N\rangle$, i.e.,

$$\langle E_{k\nu,0}^{N-1}|\psi_\nu|E_0^N\rangle=\langle E_0^N|\psi_{k\nu}^\dagger\psi_\nu|E_0^N\rangle\left[1+O\left[\frac{1}{N_f}\right]\right]\ , \tag{4.12}$$

and $E_{k\nu,0}^{N-1}\to E_0^N-\epsilon_k$. We call that part of $\rho_f(\epsilon)$ in (4.11) which results from taking only the $\alpha=0$ state for each k, $\rho_f^{(0)}(\epsilon)$. Using

$$\langle E_0^N|\psi_{k\nu}^\dagger\psi_\nu|E_0^N\rangle=\langle B_0|B_k\rangle/(N_f)^{1/2}$$

and (3.13), we obtain

$$\begin{aligned}\rho_f^{(0)}(\epsilon)&=\sum_{k\le k_f}|\langle B_0|B_k\rangle|^2\delta(\epsilon-\epsilon_k)\\&=\left|\left\langle B_0\left|\frac{1}{\epsilon-h_1}\right|B_0\right\rangle\right|^2\frac{\mathrm{Im}\tilde{\Gamma}(\epsilon-i0)}{\pi}\ ,\end{aligned} \tag{4.13}$$

with $h_1=H_B(1)+\epsilon_f-\Delta E$. Near the Fermi energy this is the only contribution of $\rho_f(\epsilon)$. The energy range over which $\rho_f(\epsilon)$ and $\rho_f^{(0)}(\epsilon)$ coincide is at least as large as the energy separation between the ground state $|B_0^{(0)}\rangle$ ($\equiv|B_0\rangle$) and the first excited state $|B_0^{(1)}\rangle$ which one obtains by solving (3.14). As discussed for the "phonon case" in Sec. V this energy separation is extremely small for a small range of ϵ_f values if $v=\lambda^2/\omega_0$ is large. For these parameter values, (4.13) presents $\rho_f(\epsilon)$ only in an extremely small energy range below ϵ_F. It is then necessary to use

$$\begin{aligned}\rho_f^{(0,1)}(\epsilon)=&\rho_f^{(0)}(\epsilon)\\&+\left|\left\langle B_0^{(1)}\left|\frac{1}{\epsilon+E_{10}-h_1}\right|B_0^{(0)}\right\rangle\right|^2\\&\times\frac{\mathrm{Im}\tilde{\Gamma}(\epsilon+E_{10})}{\pi}\ ,\end{aligned} \tag{4.14}$$

where $E_{10}=(\Delta E)_1-(\Delta E)_0$ is the lowest excitation energy to be obtained from (3.14). The f-level occupancy $n_f=\langle E_0|\hat{n}_f|E_0\rangle$ can be expressed as

$$\begin{aligned}n_f=\sum_{k\le k_f}\langle B_k|B_k\rangle=\int d\epsilon\left[-\frac{\partial}{\partial\epsilon}\left\langle B_0\left|\frac{1}{\epsilon-h_1}\right|B_0\right\rangle\right]\\\times\frac{\mathrm{Im}\tilde{\Gamma}(\epsilon-i0)}{\pi}\ .\end{aligned} \tag{4.15}$$

For a broad valence band with a constant density of states, we therefore obtain with $\tilde{\Delta}=\mathrm{Im}\tilde{\Gamma}$,

$$\rho_F(\epsilon_F)=\pi n_f^2/\tilde{\Delta}\ . \tag{4.16}$$

This is the $N_f\to\infty$ version of the generalized Friedel sum rule for our model. It should be obvious from the discussion leading to Eq. (4.14) that this sum rule is not a very useful relation if E_{10} is much smaller than the relevant electronic energies and the difference $\rho_f^{(0,1)}(\epsilon)-\rho_f^{(0)}(\epsilon)$ is not small compared to $\rho_f^{(0)}(\epsilon)$. A detailed discussion of the full spectral function will be presented in Secs. V and VI.

V. "PHONON" CASE

In this section we discuss in detail the limit of small boson frequency $\omega_0\ll\tilde{\Delta}$ and couplings λ such that we are *near the adiabatic limit* in which the electrons adjust to the motion of the oscillator instantaneously. Before we present exact numerical results for this limit, we give an approximate solution in the spirit of the Born-Oppenheimer approach for the description of the coupling of electronic and nuclear motion.[19] For that purpose it is useful to return to the spatial coordinates of the oscillator and write the Hamiltonian in (3.4) as

$$\begin{aligned}H&=H_{\mathrm{el}}+\hat{p}^2/2m+\tfrac{1}{2}c\hat{x}^2-\omega_0/2+(2m\omega_0)^{1/2}\lambda\hat{x}\cdot\hat{n}_f\\&=H(\hat{x})+\hat{p}^2/2m\ ,\end{aligned} \tag{5.1}$$

where $c=m\omega_0^2$ is the force constant. It is useful to introduce a new coupling constant $\tilde{\lambda}=\lambda/\omega_0^{1/2}$ since $\tilde{\lambda}=$const corresponds to a fixed value of the relaxation energy. The electron-phonon—coupling term in (5.1) is then given by $\sqrt{2c}\,\tilde{\lambda}\hat{x}\cdot\hat{n}_f$. If for given c and $\tilde{\lambda}$ the mass m goes to infinity, the kinetic-energy term can be treated as a small perturbation. Replacing the operator $\hat{x}$ in (5.1) by a c-number x, we write

$$H(x)=H_{\mathrm{el}}(x)+\tfrac{1}{2}cx^2-\tfrac{1}{2}(c/m)^{1/2}\ , \tag{5.2}$$

where H_{el} is of the same form as H_{el} but with an x-dependent f-level position $\epsilon_f(x)$,

$$\epsilon_f(x)=\epsilon_f+(2m\omega_0)^{1/2}\lambda x\ . \tag{5.3}$$

We now define the adiabatic electronic eigenstates $|\Phi_n(x)\rangle$,

$$H_{\mathrm{el}}(x)|\Phi_n(x)\rangle=E_n(x)|\Phi_n(x)\rangle\ , \tag{5.4}$$

and expand the exact ground state following Born and Huang as[19]

$$\langle x|E_0\rangle=\sum_n\phi_n(x)|\Phi_n(x)\rangle \tag{5.5}$$

$$\approx\phi_0(x)|\Phi_0(x)\rangle\ , \tag{5.6}$$

where $\phi_0(x)$ obeys the Schrödinger equation

$$\left[-\frac{1}{2m}\frac{d^2}{dx^2}+E_0(x)+\tfrac{1}{2}cx^2-\tfrac{1}{2}(c/m)^{1/2}\right]\phi_0(x)=\epsilon_0\phi_0(x)\ . \tag{5.7}$$

With the variational *Ansatz* (5.6), the ground-state energy is given by

$$E_0=\epsilon_0+\frac{1}{2m}\int dx\,|\phi_0(x)|^2\left\langle\frac{\partial\Phi_0}{\partial x}\middle|\frac{\partial\Phi_0}{\partial x}\right\rangle . \tag{5.8}$$

In this paper the "adiabatic approximation" means the form (5.6) introduced by Born and Huang.[19] This adiabatic approximation is different from the so-called "crude adiabatic approximation" in which, instead of (5.6), one uses

$$\langle x\,|\,E_0\rangle=\phi_0(x)\,|\,\Phi_0(x_0)\rangle$$

with x *fixed* to some value x_0 in the electronic state. In their paper, Kohn *et al.*[14] use the term "adiabatic approximation" with the meaning crude adiabatic approximation. In the crude adiabatic approximation the ground state $|E_0\rangle$ is described as *product* state $|\phi_0\rangle\,|\Phi_0(x_0)\rangle$, while, for the (Born-Huang) adiabatic approximation (5.6), this is *not* the case. To proceed, we first have to calculate the adiabatic electronic ground state. Using the same arguments as in Sec. III, the exact result in the limit $N_f\to\infty$ is of the form

$$|\Phi_0(x)\rangle=A(x)\left[|0\rangle-\sum_k\frac{\tilde{V}_k}{\epsilon_f(x)-\Delta E(\epsilon_f(x))-\epsilon_k}|k\rangle\right], \tag{5.9}$$

where

$$\Delta E(\epsilon_f(x))=E_0(x)-E_0^0$$

is determined by

$$\Delta E(\epsilon_f(x))=-\tilde{\Gamma}[\epsilon_f(x)-\Delta E(\epsilon_f(x))] , \tag{5.10}$$

and

$$A(x)=[1-n_f(\epsilon_f(x))]^{1/2}$$

with

$$n_f(\epsilon_f(x))=\langle\Phi_0(x)\,|\,\hat{n}_f\,|\,\Phi_0(x)\rangle$$

a normalization factor.

In the ground state the oscillator shows zero-point oscillations around the deepest minimum of the potential,

$$V_0(x)=E_0(x)+\tfrac{1}{2}cx^2 , \tag{5.11}$$

provided this minimum is nondegenerate and the mass is sufficiently large. The position x_0 of the minimum is determined by setting the first derivative of the potential equal to zero. Using the Hellmann-Feynman theorem and units such that $(2m\omega_0)^{1/2}=1$, this leads to

$$x_0=-(2\lambda/\omega_0)n_f(\epsilon_f+\lambda x_0) . \tag{5.12}$$

This can be compared with the exact relation

$$\langle E_0\,|\,\hat{x}\,|\,E_0\rangle=-(2\lambda/\omega_0)\langle E_0\,|\,\hat{n}_f\,|\,E_0\rangle , \tag{5.13}$$

which follows from $\langle E_0\,|\,[(b-b^\dagger),H]\,|\,E_0\rangle=0$. Note that with the units chosen above, $\hat{x}=b+b^\dagger$. Introducing a new variable n_0 by $x_0=-(2\lambda/\omega_0)n_0$ and $v=\lambda^2/\omega_0=\tilde{\lambda}^2$, the condition for the minimum of the adiabatic potential can be written as

$$n_0=n_f(\epsilon_f-2vn_0) . \tag{5.14}$$

This is exactly the same equation for n_0 as the equation for $\langle\hat{n}_f\rangle^{\text{Hartree}}$ in a mean-field approximation concerning the electron-boson coupling. The function $n_f(u)$ is a monotonic decreasing function of its argument. From (5.14) we can infer that the curves of constant n_0 in a (ϵ_f,v) plane are straight lines $v=\text{const}+\epsilon_f/2n_0$. For a qualitative graphical solution of (5.14), it is useful to work with the variable $u=\epsilon_f-2vn_0$, i.e.,

$$-(1/2v)(u-\epsilon_f)=n_f(u) . \tag{5.15}$$

A plot of $n_f(u)$ is shown in Fig. 1 for a constant conduction density of states. The energy scale is determined by $\tilde{\Delta}=\text{Im}\tilde{\Gamma}(\epsilon-i0)$ $(\epsilon<0)$. The absolute value of the slope of $n_f(u)$ has a *single* maximum occurring at $n_f=\frac{2}{3}$ (as discussed in Appendix B). For small electron-phonon coupling, i.e., small v, a unique solution to (5.15) exists because the negative slope of the straight line intersecting $n_f(u)$ is larger than the maximal negative slope of $n_f(u)$. As v is increased, multiple solutions to Eq. (5.15) first occur for a critical value v_{crit} determined by the maximum negative slope of $n_f(u)$. A straight line through the inflection point $n_f(u)$ having a slope less negative than that of $n_f(u)$ produces three solutions: The solution with $n_f=\frac{2}{3}$ then corresponds to a *maximum* of $V_0(x)$, while the two new solutions present minima of $V_0(x)$. This follows from the fact that $V_0(x)$ is dominated by the term $\frac{1}{2}cx^2$ for $x\to\infty$, or, by calculating the second derivative $V''(x_0)$, by (5.29). For $v>v_{\text{crit}}$ there is a finite interval of ϵ_f values for which double minima occur. At the lower edge of the interval the "large" n_0 minimum is the absolute minimum, while at the upper edge the small n_0 minimum is the absolute minimum. At an intermediate ϵ_f value, which can be determined by a Maxwell construction of equal area under the straight line and $n_f(u)$ between the two minima, the two minima are degenerate. At this value of n_0 there is (in the limit $m\to\infty$) a discon-

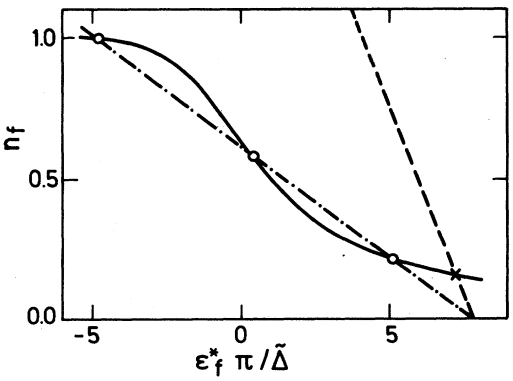

FIG. 1. f-level occupancy as a function of the f-level position for a constant conduction-band density of states in the limit of zero electron-phonon coupling ($\lambda=0$). [See (B3) for the definition of ϵ_f^*.] The intersection points with the straight lines ($v<v_c$, — — —; $v>v_c$, —·—·—·) give the f occupancy in the mean-field approximation for the electron-phonon coupling.

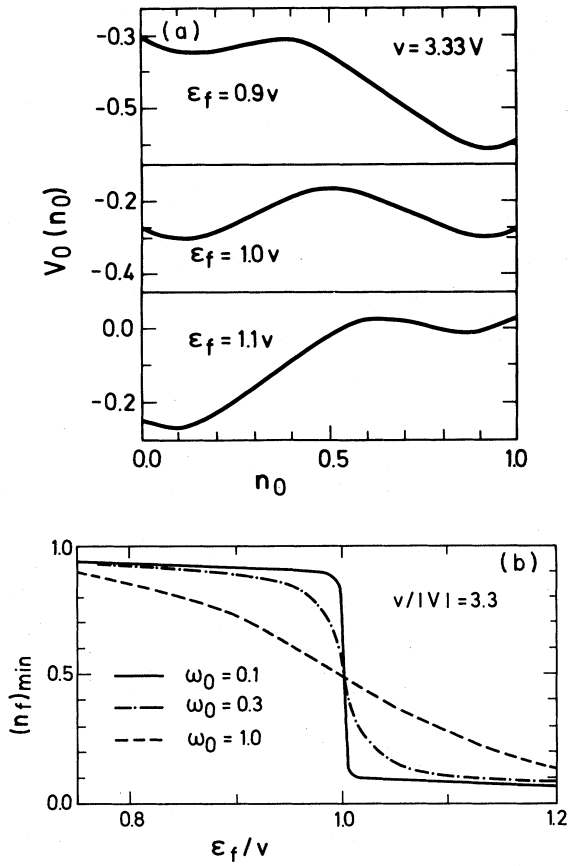

FIG. 2. (a) Adiabatic ground-state potentials V_0 as a function of the dimensionless variable $n_0=-x\omega_0/2\lambda$ for the zero-bandwidth case. (b) Exact results for the f-level occupancy as a function of the f-level position in the zero-bandwidth limit. As $v>v_{\rm crit}$, the variation of n_f with ϵ_f becomes discontinuous in the limit $\omega_0\to 0$.

tinuous change of n_0. This is shown in Fig. 2 for the zero-bandwidth limit (for a detailed discussion, see Appendix A).

In Fig. 3 we show the corresponding "$m=\infty$" phase diagram in the (ϵ_f,v) plane. It shows that the "mixed-valence regime" *shrinks drasically for increasing* v. If one would define this regime, e.g., by $0.1<n_f<0.9$, then the mixed-valence regime would shrink to the critical line above a certain v value. For finite mass m, quantum fluctuations prevent the discontinuous change of n_f. This is shown in Fig. 2(b), which shows exact numerical results using (3.14) for different values of ω_0, i.e., m. For frequencies ω_0 comparable to the relevant electronic energies, there is a *smooth* transition from n_f values of order one to small n_f values. As ω_0 is decreased the exact result approaches the discontinuous $m\to\infty$ result very rapidly. The energy range over which the transition occurs is determined by the bonding-antibonding splitting of the oscillator in the degenerate wells. In the units we use the zero-point fluctuations in a single well are of order unity. The separation of the wells follows from (5.12) and is of order $(v/\omega_0)^{1/2}$. For $v>v_{\rm crit}$ the bonding-antibonding splitting contains a factor $\exp(-\alpha^2 v/\omega_0)$, where α^2 is of order one. This explains the rapid approach to the $m\to\infty$ ($\omega_0\to 0$) first-order transition.

In Fig. 4 we show an exact phase diagram for a finite bandwidth B and a typical phonon frequency ω_0. For the hopping parameters $\tilde{V}_k$ we use

$$\pi\sum_k |\tilde{V}_k|^2\delta(\epsilon-\epsilon_k)=\tilde{\Delta}(B^2-\epsilon^2)^{1/2}/B\ ,$$

where $2B$ is the total bandwidth and the Fermi energy ϵ_F is set equal to zero. For this value of ω_0 the drastic shrinking of the mixed-valence regime with increasing v shows up in the exact solution. In the impurity model studied in this paper the occurrence of mixed-valence behavior therefore appears highly improbable for $v\gg v_{\rm crit}$. In a more realistic model, on the other hand, a mechanism may exist which pins the f level to that mixed-valence regime. The effect of the quantum fluctuations which suppress the first-order transition can already be understood within the adiabatic approximation (5.6): The oscillator wave function $\phi_0(x)$ changes *continuously* from being concentrated in one potential minimum or the other. A rigorous description of this effect can be obtained by considering the exact probability distribution of the oscillator coordinate,

$$p(x)=\langle E_0|\delta(x-\hat{x})|E_0\rangle=\langle E_0|x\rangle\langle x|E_0\rangle\ , \qquad (5.16)$$

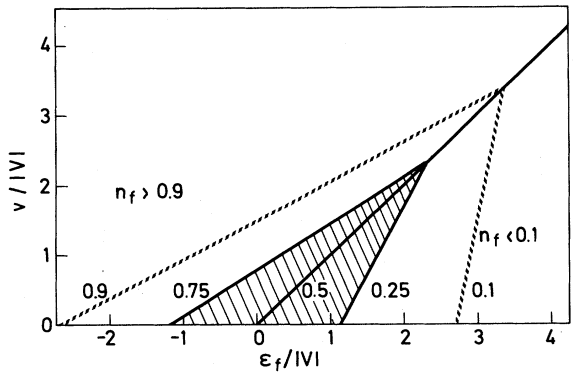

FIG. 3. "Phase diagram" for the f occupancy in the (ϵ_f,v) plane. The result shown is for the zero-bandwidth case in the limit $\omega_0\to 0$.

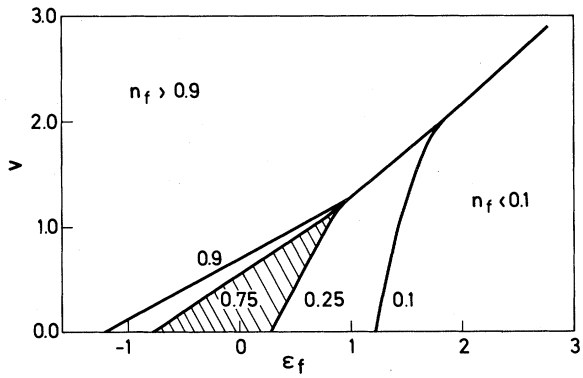

FIG. 4. Exact "phase diagram" for the f occupancy for $B=2$, $\tilde{\Delta}=1$, and $\omega_0=0.02$ eV.

which can be evaluated using Eqs. (3.19) and (3.20). It follows from (5.13) that the first moment of $p(x)$ is determined by the exact f-level occupancy,

$$\int_{-\infty}^{\infty} xp(x)dx = -(2\lambda/\omega_0)\langle E_0 \mid \hat{n}_f \mid E_0 \rangle \ . \tag{5.17}$$

Figure 5 shows the adiabatic potential-energy curve as a function of $n = -(\omega_0/2\lambda)x$ for the finite-bandwidth case. The parameters are chosen such that the minimum to the right ($n \approx 0.98$) is the deeper one. In the limit $\omega_0 \to 0$ one is therefore in the "spin"-fluctuation limit. The figure also shows the exact probability distribution (5.16). For $\omega_0 = 0.075$ eV, the "lattice" is still essentially confined to the right-hand well and the exact f-level occupancy is 0.952. For the same value of v, but for $\omega_0 = 0.1$, the quantum fluctuations change the model qualitatively: There is almost an equal probability of finding the "lattice" in either well and the occupancy of the f level is 0.565. This mixed-valence behavior results from a highly correlated motion of the oscillator and the f occupancy. This is shown clearly by the dotted curve in Fig. 5, which shows

$$p_0(x) = \langle E_0 \mid (1-\hat{n}_f) \mid x \rangle \langle x \mid E_0 \rangle \ , \tag{5.18}$$

where $p_0(x)dx$ describes the conditional probability for the nuclear coordinate to be in the interval $[x, x+dx]$ knowing that the f-level occupancy is zero. The *total* probability for the "lattice" being in the left-hand well is strongly correlated with the occurrence of zero f occupancy. The exact results for $p(x)$ and $p_0(x)$ can be easily understood by assuming that the adiabatic approximation (5.6) for the ground state is a good approximation. From (5.6) one obtains the approximate relations

$$p^{\mathrm{ad}}(x) = \mid \phi_0(x) \mid^2 \tag{5.19}$$

and

$$p_0^{\mathrm{ad}}(x) = \mid \phi_0(x) \mid^2 [1 - n_f(\epsilon_f(x))] \ . \tag{5.20}$$

Therefore, even without calculating $\phi_0(x)$ by a numerical integration of (5.7), we can test the accuracy of the adiabatic approximation (5.6) by noting that, according to (5.19) and (5.20), the ratio $\gamma_{\omega_0}(x) = p_0(x)/p(x)$ should be *independent* of ω_0. Figure 6 shows that $\gamma_{0.075}(x)/\gamma_{0.1}(x)$ deviates from 1 by less than 15%. Since the adiabatic ground-state potential $V_0(x)$ shown in Fig. 5 is known only numerically, we have not calculated the corresponding $\phi_0(x)$ to compare Eqs. (5.16) and (5.18) directly with (5.19) and (5.20). This is done for the zero-bandwidth case in Fig. 7, for which the adiabatic ground-state potential is known analytically (Appendix A). Figure 7 shows that the adiabatic approximation (5.6) provides a qualitatively correct description for the parameters considered.

The mixed-valence behavior for $v > v_{\mathrm{crit}}$ is very different from the mixed-valence behavior for $v \lesssim v_{\mathrm{crit}}$. For $v > v_{\mathrm{crit}}$ the adiabatic potential $V_0(x)$ has only a single minimum at x_0, and the zero-point fluctuations in the well, determined by $V''(x_0)$ and m, are small. In the limit $m \to \infty$, a second-order transition occurs at $v = v_{\mathrm{crit}}$, and, for $v > v_{\mathrm{crit}}$, the distance of the two minima essentially determines the fluctuation

$$\Delta x = (\langle E_0 \mid \hat{x}^2 \mid E_0 \rangle - \langle E_0 \mid \hat{x} \mid E_0 \rangle^2)^{1/2}$$

in a mixed-valence situation. The behavior of Δx through the transition is shown in Fig. 8 for the zero-bandwidth case. Again, one can see how the quantum fluctuations smear out the second-order transition occurring in the limit $m \to \infty$ ($\omega_0 \to 0$).

The difference in the mixed-valence behavior for $v < v_{\mathrm{crit}}$ and $v > v_{\mathrm{crit}}$ can be clearly seen in the one-particle

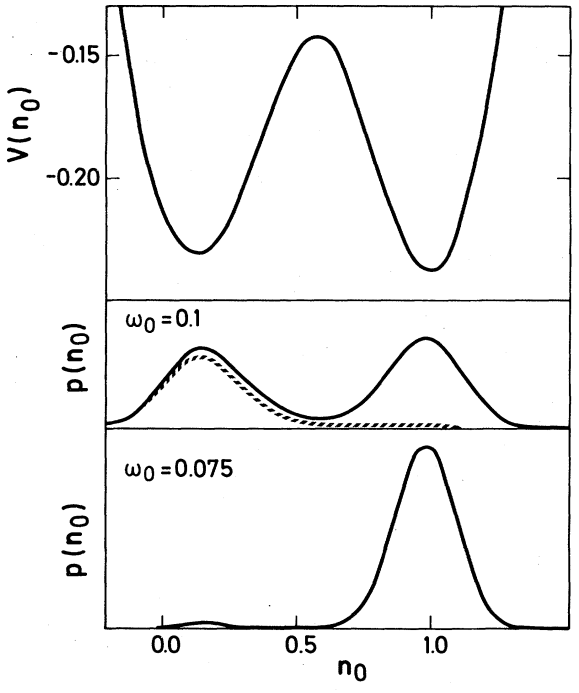

FIG. 5. Upper part shows the adiabatic potential-energy curve as a function of $n_0 = -x\omega_0/2\lambda$ for $B = 2$, $\tilde{\Delta} = 1$, $v = 1.62$, and $\epsilon_f = 1.385$. The solid curves in the lower part of the figure show the exact probability distribution $p(n_0)$ of the oscillator coordinate. The dotted curve shows the exact probability density $p_0(n_0)$ for the oscillator coordinate corresponding to zero f-level occupancy.

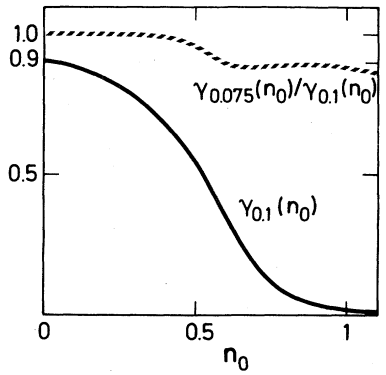

FIG. 6. Ratio $\gamma_{\omega_0}(n) = p_0(n)/p(n)$ (see Fig. 5 for the definition of p and p_0) is shown for $\omega_0 = 0.1$ (solid curve). The dotted curve shows the exact result for the ratio $\gamma_{0.075}(n_0)/\gamma_{0.1}(n_0)$, which is independent of n_0 (and equal to 1) in the adiabatic approximation.

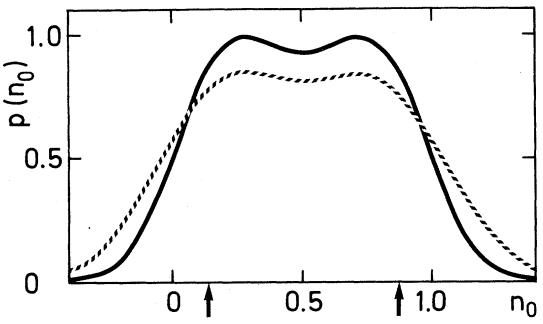

FIG. 7. Solid curve shows the exact result for the probability distribution $p(n_0)$ in the zero-bandwidth case for $\tilde{V}=1$, $v=3$, and $\epsilon_f=v$ ("symmetric case") for $\beta=\lambda^2/\omega_0^2=10$. The dashed curve shows the corresponding result $p^{\rm ad}(n_0)=|\phi_0(n_0)|^2$ in the adiabatic approximation. The arrows indicate the positions for the minima of the adiabatic potential-energy curve, which is symmetric with respect to $n_0=\frac{1}{2}$.

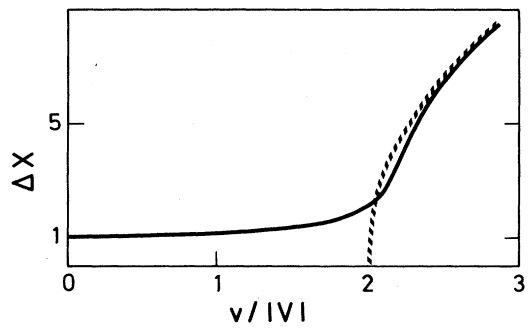

FIG. 8. Solid curve shows the exact result for the fluctuation $\Delta x=(\langle E_0|\hat{x}^2|E_0\rangle-\langle E_0|\hat{x}|E_0\rangle^2)^{1/2}$ in the zero-bandwidth case as a function of v for $\tilde{V}=1$, $\epsilon_f=v$, and $\omega_0=0.02$. The dotted line shows the separation of the two minima of the adiabatic potential-energy curve.

Green's function $g_f^<(z)$ calculated in Sec. IV. Before we present exact numerical results using (4.9), we introduce the adiabatic approximation for the ground state in order to obtain an approximate analytical result for $g_f^<(z)$,

$$g_f^<(z)=N_f\int dx\,dx'\,\langle E_0|x'\rangle\psi_v^\dagger\left\langle x'\left|\frac{1}{z-E_0+H}\right|x\right\rangle \times\psi_v\langle x|E_0\rangle\ . \tag{5.21}$$

In the narrow-band limit, the exact spectrum shows sharp phonon satellites when lifetime broadening is neglected, i.e., when z approaches the real axis. In the broadband case this discrete structure is lost because of the continuous spectrum of electronic excitations. There are, therefore, two reasons why the phonon fine structure of the spectrum usually cannot be resolved in the systems we have in mind. We therefore first consider an approximation which produces the correct "broadened" spectrum ($|\mathrm{Im}(z)|>\omega_0$) in the limit of small ω_0. In this approximation we neglect the kinetic-energy term of the oscillator, i.e., we replace H by $H(x)$ in (5.2), where $H(x)$ is defined in (5.1). Since the neglected term is proportional to ω_0, the "normal" phonon broadening of the spectral lines, which turns out to be of order $\lambda\sim(\omega_0)^{1/2}$, is still described correctly to order $(\omega_0)^{1/2}$. With this approximation, the resolvent matrix element in (5.21) is diagonal and one integration can be carried out. Using the adiabatic approximation (5.6) for $\langle x|E_0\rangle$, we obtain the approximate expression $\tilde{g}(z)$ for $g_f^<(z)$,

$$\tilde{g}(z)=N_f\int|\phi_0(x)|^2\left\langle\Phi_0(x)\left|\psi_v^\dagger\frac{1}{\tilde{z}(x)-E_0+H_{\rm el}(x)}\psi_v\right|\Phi_0(x)\right\rangle$$
$$=\int|\phi_0(x)|^2 g^<_{\epsilon_f(x)}(\tilde{z}(x))dx\ , \tag{5.22}$$

where

$$\tilde{z}(x)=z+V_0(x)-E_0\ ,$$

and $g^<_{\epsilon_f(x)}$ is the purely electronic f-level Green's function with the f level at $\epsilon_f(x)=\epsilon_f+\lambda x$. In $\tilde{z}(x)$ we have dropped the constant shift $\omega_0/2$ which appears in (5.2) since (5.22) is only correct to order $\omega_0^{1/2}$. The spectral function $\tilde{\rho}(\epsilon)=\mathrm{Im}[\tilde{g}(\epsilon-i0)]/\pi$ is therefore given by the corresponding electronic spectral function $\rho^<_{\epsilon_f(x)}(\epsilon)$ *weighted* by the ground-state probability distribution $|\phi_0(x)|^2=p^{\rm ad}(x)$,

$$\tilde{\rho}(\epsilon)=\int|\phi_0(x)|^2\rho^<_{\epsilon_f(x)}(\epsilon+V_0(x)-E_0)dx\ . \tag{5.23}$$

In the limit $\omega_0\to0$ the weighting function $p^{\rm ad}(x)$ goes over to a δ function $\delta(x-x_0)$ if the deepest minimum of $V_0(x)$ is nondegenerate. As the ground-state energy E_0 goes over to $V_0(x_0)$ in the limit $\omega_0\to0$ ($v=$const), one obtains

$$\mathrm{Im}[g_f^<(\epsilon-i0)]/\pi=\rho^<_{\hat{\epsilon}_f}(\epsilon)\ , \tag{5.24}$$

with $\hat{\epsilon}_f=\epsilon_f-2n_0v$. This result, which holds asymptotically in the limit $\omega_0\to0$, can also be obtained using a Hartree-type mean-field description of the electron-phonon–interaction term. The qualitative features of the spectral function on the right-hand side (rhs) of (5.24) has been discussed in detail in Ref. 6. For $\hat{\epsilon}_f$ near the Fermi energy ϵ_F and a broad valence band, $\rho^<_{\hat{\epsilon}_f}(\epsilon)$ shows a rise at ϵ_F and a "plateau" below $\hat{\epsilon}_f$, if $\hat{\epsilon}_f$ is of the order $\tilde{\Delta}=\mathrm{Im}\tilde{\Gamma}(\hat{\epsilon}_f-i0)$ below the Fermi energy $\epsilon_F=0$. This is the mixed-valence regime. In the spin-fluctuation regime $-\hat{\epsilon}_f\gg\tilde{\Delta}$, there is a Lorentzian peak of width $\tilde{\Delta}$ near $\hat{\epsilon}_f$ and a very sharp rise near the Fermi energy. This "Kondo peak" has very little weight if $\hat{\epsilon}_f$ is sufficiently far below the Fermi energy. To see how the phonon broadens the spectrum, in particular, the "Kondo peak" for finite ω_0, one must go beyond the approximation (5.24). We use the spectral representation

$$\rho^{<}_{\epsilon_f(x)}(\epsilon+V_0(x)-E_0)=\sum_i R_i(x)\delta(\epsilon+V_0(x)-E_0-[E_0^N(x)-E_i^{N-1}(x)]) ,$$

and expand the argument of the δ function to linear order around the minimum. Using the Hellmann-Feynman theorem the expectation value

$$n_i^{N-1}=\langle \Phi_i^{N-1}(x_0)\,|\,\hat{n}_f\,|\,\Phi_i^{N-1}(x_0)\rangle$$

enters. Then the x integration in (5.23) can be carried out,

$$\tilde{\rho}(\epsilon)=\sum_i R_i(x_0+f_i(\epsilon))c_i\exp[-\alpha(f_i(\epsilon))^2] , \tag{5.25}$$

with

$$f_i(\epsilon)=\frac{\epsilon-[E_0^N(x_0)-E_i^{N-1}(x_0)]}{\lambda(n_0^N-n_i^{N-1})} , \tag{5.26}$$

$$\alpha=\frac{1}{2}\left[1+2v\frac{dn_0(\hat{\epsilon}_f)}{d\hat{\epsilon}_f}\right] , \tag{5.27}$$

and

$$c_i=(\alpha/\pi)^{1/2}/\,|\,\lambda(n_0^N-n_0^{N-1})\,|\ . \tag{5.28}$$

Here, we have used the fact that ϕ_0 is a Gaussian centered around x_0 with a width determined by

$$V_0''(x_0)=\frac{\omega_0}{2}\left[1+2v\frac{dn_0(\hat{\epsilon}_f)}{d\hat{\epsilon}_f}\right] . \tag{5.29}$$

From (5.25)—(5.27) we see that the vibrational width is proportional to $\lambda=(v\omega_0)^{1/2}$ and to the difference in the slope of the adiabatic potential-energy curves $V_0^N(x)$ and $V_i^{N-1}(x)$ at the point x_0. To apply these results to our specific model, we must use the explicit expression for $\rho^{<}_{\epsilon_f(x)}(\epsilon)$, given previously,[5,6] which can also be obtained from (4.9),

$$\rho^{<}_{\epsilon_f(x)}(\epsilon)=[1-n_f(\epsilon_f(x))]\sum_{k\le k_f}\frac{|\,\tilde{V}_k\,|^2}{[\epsilon_f(x)-\Delta E(\epsilon_f(x))-\epsilon_k]^2}$$

$$\times\frac{1}{\pi}\mathrm{Im}\left[\frac{1}{\epsilon-i0-\epsilon_k-\Delta E(\epsilon_f(x))-\tilde{\Gamma}[\epsilon-i0-\epsilon_k-\Delta E(\epsilon_f(x))+\epsilon_f(x)]}\right] . \tag{5.30}$$

For every value of k, the spectrum in (5.30) consists of a pole at $\epsilon=\epsilon_k$ and a quasicontinuous part starting at an energy $\epsilon_f(x)-\Delta E(\epsilon_f(x))$ below ϵ_k. As the pole is at ϵ_k *independently of the value of* x, this pole part obtains no phonon broadening of order $\lambda=(v\omega_0)^{1/2}$. In the narrow-band limit $B\to 0$, the continuous part of (5.30) shrinks to an additional pole contribution. This peak has a phonon broadening described approximately by (5.25)—(5.28). A comparison with the exact numerical solution is shown in Fig. 9. As discussed above, there is no phonon broadening of order $(v\omega_0)^{1/2}$ of the peak at threshold. (We have introduced a lifetime broadening $y=0.05$ for numerical convenience for the exact calculation.) Except for one electron at the Fermi level missing in the infinite reservoir of valence electrons, the corresponding adiabatic final state is identical to the initial state, as discussed in Sec. IV, and leads, therefore, to the *same* adiabatic potential $V_0(x)$. In order to examine the fine structure of the peak at threshold on an energy scale ω_0, one must go beyond the approximation leading to (5.22). According to the exact spectral representation (4.11), there are (if the weight factor differs from zero) contributions to the spectrum from *all* excited states $|\,E_{kv,\alpha}^{N-1}\rangle\approx\psi_{kv}|\,E_\alpha^N\rangle$ with $\alpha\neq 0$. These are automatically included in the exact solution (4.9). For small ω_0 these low-lying excited states can be described approximately in the adiabatic approximation, in analogy to (5.6),

$$\langle x\,|\,E_\alpha^N\rangle\approx\phi_\alpha(x)\,|\,\Phi_0(x)\rangle , \tag{5.31}$$

where the $\phi_\alpha(x)$ are the excited states for the motion in the adiabatic ground-state potential $V_0(x)$ which can be obtained by solving the Schrödinger equation (5.7). The spectral weight factors in (4.11) are then given by

$$|\,\langle E_{kv,\alpha}^{N-1}\,|\,\psi_v\,|\,E_0^N\rangle\,|^2\approx\left|\int\phi_\alpha^*(x)\phi_0(x)\times\langle\Phi_0(x)\,|\,\psi_{kv}^\dagger\psi_v\,|\,\Phi_0(x)\rangle dx\right|^2 . \tag{5.32}$$

Because of the electronic matrix element in the integrand, the orthogonality of ϕ_α and ϕ_0 cannot be used to argue that the matrix element vanishes for $\alpha\neq 0$. The total weight in the vibrationally *excited* states for fixed k is given by

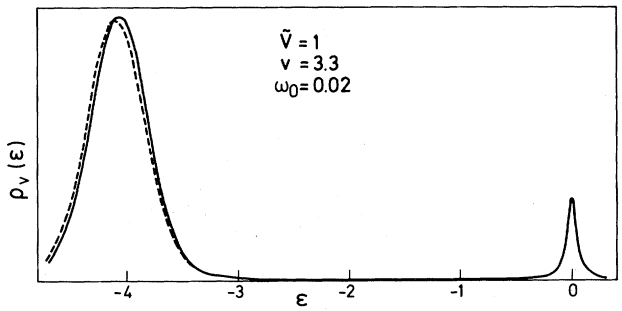

FIG. 9. Comparison of the exact f-level spectral function (solid curve) with the approximate result (5.25) in the zero-bandwidth case. A lifetime broadening $y=0.05$ has been used in the calculation and the phonon fine structure of the exact result is therefore not resolved.

$$\sum_{\alpha\,(\neq 0)} |\langle\phi_\alpha|f_k(\hat{x})|\phi_0\rangle|^2=\langle\phi_0|[f_k(\hat{x})]^2|\phi_0\rangle - [\langle\phi_0|f_k(\hat{x})|\phi_0\rangle]^2 , \quad (5.33)$$

with

$$f_k(x)=\langle\Phi_0(x)|\psi^\dagger_{kv}\psi_v|\Phi_0(x)\rangle = \frac{\tilde{V}_k[1-n_f(\epsilon_f(x))]}{\epsilon_k+\Delta E(\epsilon_f(x))-\epsilon_f(x)} . \quad (5.34)$$

For the case when $V_0(x)$ has a *nondegenerate* deepest minimum at $x=x_0$, we expand $f_k(x)$ to order $(x-x_0)^2$ around x_0 to estimate the rhs of (5.33),

$$\sum_{\alpha\,(\neq 0)} |\langle\phi_\alpha|f_k(\hat{x})|\phi_0\rangle|^2 = \lambda^2\left[\frac{df_k}{d\hat{\epsilon}_f}\right]^2\langle\phi_0|(\hat{x}-x_0)^2|\phi_0\rangle(2m\omega_0)+O(\lambda^3) . \quad (5.35)$$

The ground-state wave function $\phi_0(x)$ is a Gaussian and the width is determined by $V_0''(x_0)$ [Eq. (5.29)]. The mean-square deviation $\langle\phi_0|(x-x_0)^2|\phi_0\rangle$ multiplied by $2m\omega_0$ is therefore of order unity. In the zero-bandwidth limit one obtains, using (A2) and (A3),

$$(df/d\hat{\epsilon}_f)^2=[4n_f(1-n_f)(2n_f-1)]^2/\tilde{V}^2 .$$

The weight in the first phonon satellite of the peak at threshold is therefore smaller than $\omega_0 v/\tilde{V}^2$. Inserting the numbers corresponding to Fig. 9 we find that the weight of the first phonon satellite is a factor of $\frac{1}{20}$ smaller than the main peak. Similarly, one can show that there are strongly-energy-dependent but small corrections to the Kondo peak at threshold, as given by (5.24), as long as $v\omega_0/\tilde{\Delta}^2$ is smaller than 1.

Figure 10 shows a comparison of the exact calculation of $\mathrm{Im}g_f^<(\epsilon-i0)$, using (4.9), with the "mean-field" result $\rho^<_{\hat{\epsilon}_f}(\epsilon)$. For calculational purposes, we have introduced a lifetime broadening $y=\mathrm{Im}(z)=0.1$. The coupling constant λ is chosen such that v is approximately two-thirds of the critical value. The agreement between the approximate and the exact result is very good. In the narrow mixed-valence regime *above* v_{crit}, the spectra are very different from mixed-valence spectra below v_{crit}. Above v_{crit}, mixed-valence behavior occurs when the two minima of the adiabatic potential $V_0(x)$ are (almost) degenerate: $V_0'(x_1)=V_0'(x_2)=0$ and $V_0(x_1)\approx V_0(x_2)$. As shown in Fig. 5, there is then a finite probability of finding the "lattice" in either of the wells. In the adiabatic approximation this leads to a finite-probability amplitude $\phi_0(x)$ in both wells. From (5.23) it therefore follows that the corresponding spectrum is a *superposition of two spectra.* In an approximation analogous to (5.23) which neglects the zero-point fluctuation *in* the wells, we obtain

$$\frac{1}{\pi}\mathrm{Im}g_f^<(\epsilon-i0)=w_1\rho^<_{\hat{\epsilon}_{f1}}(\epsilon)+w_2\rho^<_{\hat{\epsilon}_{f2}}(\epsilon) , \quad (5.36)$$

with

$$w_i=\int_i|\phi_0(x)|^2dx , \quad (5.37)$$

where the integration is over the range of the ith well and $\hat{\epsilon}_{fi}=\epsilon_f+\lambda x_i$. The zero-point fluctuations in the well can be included by replacing each of the ρ's in (5.36) by an expression of the type of (5.25). The discussion of the broadening of order ω_0 of the Kondo peak for a nondegenerate deepest minimum [Eqs. (5.33)–(5.35)] must be modified in the $v>v_{\mathrm{crit}}$ mixed-valence region. The lowest excitation energy is then given by the bonding-antibonding splitting in the double well, which contains the small factor $\exp(-v/\omega_0)$. Then the rhs of (5.33) is *not* of order λ^2 if the values of $f_k(x)$ *differ* at the two (almost) degenerate minima. From the symmetry of $(df/d\epsilon_f)^2$ around $n_f=\frac{1}{2}$, it follows that the two values of f are the same in the zero-bandwidth limit if the minima are degenerate. This is not the case for $B\neq 0$, i.e., for a finite B there is an appreciable weight corresponding to an antibonding final state. This spectral weight "almost" extends to the Fermi energy for small ω_0 as the bonding-antibonding splitting vanishes exponentially in the limit $\omega_0\to 0$. This is the reason why we have introduced the additional term (4.14) in our exact discussion of the spectral function near threshold. If one adds the bonding and the antibonding contributions, neglecting their small energy separation, one returns to (5.36) and (5.37) apart from a correction of order λ^2,

$$|\langle\phi_0|f_k(x)|\phi_0\rangle|^2+|\langle\phi_1|f_k(x)|\phi_0\rangle|^2 = \langle\phi_0|[f_k(x)]^2|\phi_0\rangle-\sum_{\alpha\,(\neq 0,1)}|\langle\phi_\alpha|f_k(x)|\phi_0\rangle|^2 , \quad (5.38)$$

where $|\phi_1\rangle$ is the antibonding state and the sum over α excludes the bonding states and one antibonding state. The first term on the rhs of (5.38) is what is obtained from (5.36) and the sum only gives a contribution of order λ^2 because $|\phi_\alpha\rangle$ is orthogonal to ϕ_0 *and* ϕ_1.

Figure 11 shows the exact spectrum for a $v>v_{\mathrm{crit}}$ mixed-valence case. The lifetime broadening is chosen sufficiently small in order to resolve the main vibrational structure. The bandwidth was chosen such that $\rho^<_{\hat{\epsilon}_f(x_2)}(\epsilon)$ has a split-off peak below the bottom of the band. where

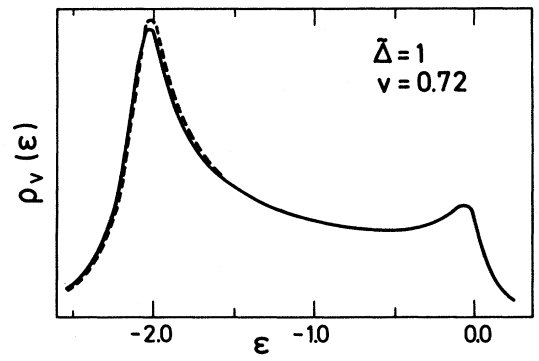

FIG. 10. Comparison of the exact result for the f-level spectral function (solid curve) with the "mean-field" result $\rho^<_{\hat{\epsilon}_f}(\epsilon)$ (dotted curve) for $B=2$. ($\hat{\epsilon}_f=1.24$.)

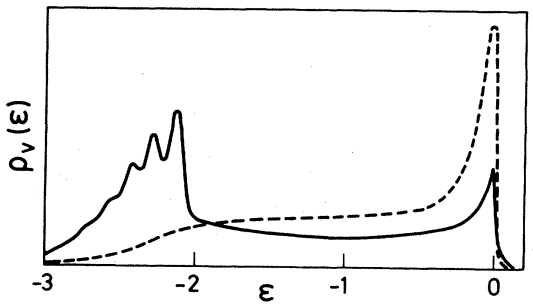

FIG. 11. Solid curve shows the f-level spectral function for $\tilde{\Delta}=1$, $v=1.62$, $\epsilon_f=1.39$, $\omega_0=0.1$, and $B=2$. The dotted curve shows the mean-field result with the f-level position adjusted to yield the same f-level occupancy ($n_f=0.55$).

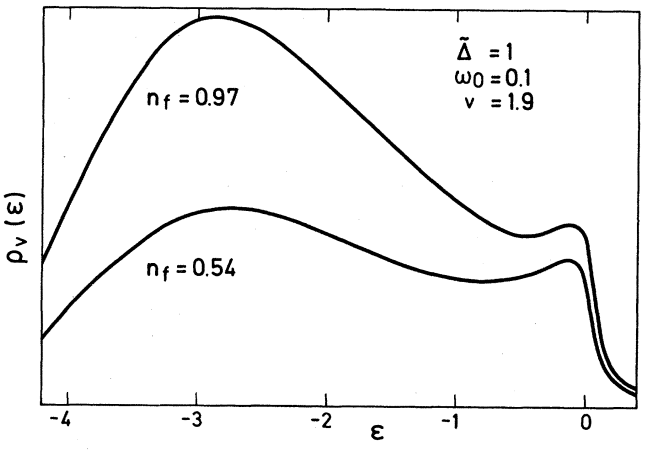

FIG. 12. Exact results for the f-level spectral function for v substantially larger than $v_{\rm crit}$ for $B=4$. The f-level position is only slightly changed from $\epsilon_f=1.560$ ($n_f=0.97$) to $\epsilon_f=1.565$ ($n_f=0.54$). The weight of the "Lorentzian" peak near -3 is changed drastically but the shift is very small.

$\hat{\epsilon}_f(x_2)$ is the adiabatic f-level position corresponding to the $n_0\approx 1$ (spin-fluctuation) minimum. The exact spectrum differs, due to its superposition character, qualitatively from the $v=0$ spectrum shown, for which the same value of the coupling $\tilde{\Delta}$ has been used, and the f-level position has been adjusted to yield the same f-level occupancy as for the $v>v_{\rm crit}$ spectrum. Owing to the finite lifetime broadening, the fine structure of the Kondo peak is not resolved. With the use of (5.36) a simple qualitative discussion of the spectrum is possible when the critical line $v_c(\epsilon_f)\approx\epsilon_f$ is crossed for $v\gg v_{\rm crit}$ by changing ϵ_f by an energy of the order of the bonding-antibonding splitting. Then the values of $\hat{\epsilon}_f=\epsilon_f-2nv$ corresponding to the two minima are $\hat{\epsilon}_{f1}\approx v$ and $\hat{\epsilon}_{f2}\approx -v$. The integrated weight (up to the Fermi energy) of $\rho^<_{\hat{\epsilon}_{f1}}(\epsilon)$ is very small because $n_1\approx 0$, while $\rho^<_{\hat{\epsilon}_{f2}}(\epsilon)$ integrates to $n_2\approx 1$. To a good approximation, the spectrum is therefore given by

$$\frac{1}{\pi}\mathrm{Im}g_f^<(\epsilon-i0)=w_2\rho^<_{\hat{\epsilon}_{f2}}(\epsilon)\ . \tag{5.39}$$

For $v\gg v_{\rm crit}\sim\tilde{\Delta}$, the spectral function $\rho^<_{\hat{\epsilon}_{f2}}(\epsilon)$ has almost all of its weight in a Lorentzian peak of *width* $\tilde{\Delta}$ at $\epsilon\sim\hat{\epsilon}_{f2}\approx -v$ (in the broadband case, $B\gg v$). If one increases ϵ_f from values on one side of the critical line (spin-fluctuation case) to a value on the other side of the line ("empty"-f-level case), w_2 changes very rapidly from 1 to 0 while the position of the peak *remains at* $\epsilon\approx -v$. Going through the "transition" does not change the shape of the spectrum but only the total weight. This happens because the transition is first order: The positions of the minima of $V_0(x)$ are practically unchanged during the transition; only the role of the deepest minimum switches from one to the other.

In a system *without* coupling to phonons, the variation of n_f from the spin-fluctuation limit $n_f\approx 1$ to the empty-f-level case $n_f\approx 0$ happens when ϵ_f moves from below the Fermi energy to an energy above the Fermi energy. The relevant energy scale is given by $\tilde{\Delta}$. In the $v\gg v_{\rm crit}$ mixed-valence regime the transition occurs when ϵ_f changes by an energy of the order of the bonding-antibonding splitting, i.e., of order $\tilde{\Delta}\exp(-v/\omega_0)$. One way to interpret this rapid transition is to say that the bare $\tilde{\Delta}$ is renormalized to $\bar{\Delta}\equiv\tilde{\Delta}\exp(-v/\omega_0)$. While this interpretation can be considered useful to describe some ground-state properties,[10] it is incorrect to assume that this automatically leads to a renormalization of the width of the one-particle spectrum. Here, highly excited states also enter and the spectrum is completely dominated by the Lorentzian peak having the *unrenormalized width* $\tilde{\Delta}$. Exact results for the spectrum for v substantially larger than $v_{\rm crit}$ are shown in Fig. 12. They agree with the qualitative discussion given above.

From Figs. 9–11 and further spectra that we have calculated, we conclude that the simple "mean-field" approximation (5.24) for the spectrum works reasonably well for $\beta=v/\omega_0\gg 1$ in the "phonon case," except in the narrow $v>v_{\rm crit}$ mixed-valence region, where it fails badly, in contrast to the superposition approximation (5.36) which allows a simple description of the transition region.

VI. PLASMON CASE

In this section we describe the opposite limit of large frequency, $\omega_0\gg\tilde{\Delta}$. This is typically the case when the model (2.1) is supposed to describe the coupling to plasmons.[15–17] As there are three additional energies B, ϵ_f, and v in the problem, one must specify how ω_0 relates to these other energies. From approximate solutions of models similar to (2.1), it is known[12] that one must distinguish, in particular, the cases $\omega_0\gg B$ and $\omega_0\ll B$. Realistically, the coupling constant λ in the plasmon case is such that a perturbational treatment in the electron-plasmon–coupling constant λ is sufficient. For the case $\omega_0\gg B$ it is possible to work out an analytical approximation even for values of $\beta=v/\omega_0=\lambda^2/\omega_0^2$ larger than 1. This is presented in the following. The bandwidth B enters the ground-state calculation [Eq. (3.14)] via the function $\tilde{\Gamma}(z)$ [Eq. (3.15)]. For z on the positive real axis, $\tilde{\Gamma}$ is real and decays like $\tilde{V}^2/z$ for $z\gg B$, where $\tilde{V}$ is defined as $\tilde{V}^2=\sum_k|\tilde{V}_k|^2\sim\tilde{\Delta}B$. If $\bar{\epsilon}_f-\Delta E\ll\omega_0$, which holds for $\omega_0\gg\tilde{\Delta}$ in the mixed-valence and spin-fluctuation limits, and for $\bar{\epsilon}_f\ll\omega_0$ if $\bar{\epsilon}_f$ is above the Fer-

mi energy ($\epsilon_F=0$), we can therefore make the replacement

$$\tilde{\Gamma}[\epsilon_f-\Delta E+H_B(1)]\approx\tilde{\Gamma}(\bar{\epsilon}_f-\Delta E)\,|\,\tilde{0}\rangle\langle\tilde{0}\,|\ , \tag{6.1}$$

with

$$\bar{\epsilon}_f=\epsilon_f-\lambda^2/\omega_0\ . \tag{6.2}$$

Equation (3.14) can then be written in the form

$$|\,B_0\rangle=\tilde{\Gamma}(\bar{\epsilon}_f-\Delta E)\frac{1}{H_B(0)-\Delta E}\,|\,\tilde{0}\rangle\langle\tilde{0}\,|\,B_0\rangle\ . \tag{6.3}$$

If we multiply this equation from the left with $\langle\tilde{0}\,|$, we obtain an equation for ΔE,

$$1=\tilde{\Gamma}(\bar{\epsilon}_f-\Delta E)\left\langle\tilde{0}\left|\frac{1}{H_B(0)-\Delta E}\right|\tilde{0}\right\rangle\ . \tag{6.4}$$

This simplifies further, if we assume $|\,\bar{\epsilon}_f\,|\ll\omega_0$, i.e., if ω_0 is the largest of *all* energies appearing in the problem. Then we can insert the eigenstates $|\,n\,\rangle_B$ of $H_B(0)$ in (6.4) and keep only the ground-state term

$$\Delta E=-\,|\,\langle\tilde{0}\,|\,0\rangle\,|^2\tilde{\Gamma}(\bar{\epsilon}_f-\Delta E)\ . \tag{6.5}$$

This equation for the ground-state-energy shift ΔE is of the same form as in the purely electronic problem, but with renormalizations $\epsilon_f\to\bar{\epsilon}_f=\epsilon_f-v$ and ($\beta=v/\omega_0=\lambda^2/\omega_0^2$)

$$\tilde{\Gamma}(z)\to\,|\,\langle\tilde{0}\,|\,0\rangle\,|^2\tilde{\Gamma}(z)=e^{-\beta}\tilde{\Gamma}(z)=\bar{\Gamma}(z)\ , \tag{6.6}$$

which correspond to the renormalization $\tilde{V}_k\to\tilde{V}_k e^{-\beta/2}\equiv\bar{V}_k$. A different simplification of (6.4) occurs if the f level is much further below the bottom of the band than ω_0, i.e., $-\bar{\epsilon}_f\gg\omega_0\gg B$. Then one obtains the result (6.5), but *without* the renormalization factor $|\,\langle\tilde{0}\,|\,0\rangle\,|^2$. This limit will be further discussed in Sec. VII.

We next calculate the valence Green's function for the case when ω_0 is the largest energy in the problem. In that limit, $|\,B_0\rangle$ in Eq. (6.3) is of the form $|\,B_0\rangle=b_0\,|\,0\rangle_B$ and the $|\,B_k\rangle$ which enter the calculation of $g_f^<(z)$ in (4.9) are given by

$$|\,B_k\rangle=b_0\frac{\tilde{V}_k\langle\tilde{0}\,|\,0\rangle}{\epsilon_k+\Delta E-\bar{\epsilon}_f}\,|\,\tilde{0}\rangle\ . \tag{6.7}$$

If this expression is used in (4.9), we obtain

$$g_f^<(z)=(1-n_f)\sum_{k\le k_f}\frac{|\,\bar{V}_k\,|^2}{(\epsilon_k+\Delta E-\bar{\epsilon}_f)^2}\times\langle\tilde{0}\,|\,[z-\Delta E-\epsilon_k+H_B(0)-\tilde{\Gamma}(z-h_k)]^{-1}\,|\,\tilde{0}\rangle\ , \tag{6.8}$$

with h_k defined in (4.10). The treatment of the resolvent matrix element in (6.8) now depends on the z values considered. For $z=\epsilon\pm iy$ and $|\,\epsilon\,|\ll\omega_0$, $|\,y\,|\ll\omega_0$, we write, similar to (6.1),

$$\tilde{\Gamma}(z-h_k)\approx\tilde{\Gamma}(z-\epsilon_k-\Delta E+\bar{\epsilon}_f)\,|\,\tilde{0}\rangle\langle\tilde{0}\,|\ , \tag{6.9}$$

which acts like a separable perturbation in the resolvent matrix. Using the well-known algebra for treating separable perturbations, one obtains

$$\langle\tilde{0}\,|\,[z-\Delta E-\epsilon_k+H_B(0)-\tilde{\Gamma}(z-h_k)]^{-1}\,|\,\tilde{0}\rangle=\frac{g_{00}(z-\epsilon_k)}{1-\tilde{\Gamma}(z-\epsilon_k-\Delta E+\bar{\epsilon}_f)g_{00}(z-\epsilon_k)}\ , \tag{6.10}$$

with

$$g_{00}(z-\epsilon_k)=\langle\tilde{0}\,|\,[z-\epsilon_k-\Delta E+H_B(0)]^{-1}\,|\,\tilde{0}\rangle\approx\frac{|\,\langle 0\,|\,\tilde{0}\rangle\,|^2}{z-\epsilon_k-\Delta E}\ . \tag{6.11}$$

The "small-z" result for $g_f^<(z)$ therefore reads

$$g_f^<(z)=(1-n_f)\sum_{k\le k_f}\frac{|\,\bar{V}_k\,|^2}{(\epsilon_k+\Delta E-\bar{\epsilon}_f)^2}\times\frac{|\,\langle 0\,|\,\tilde{0}\rangle\,|^2}{z-\epsilon_k-\Delta E-\bar{\Gamma}(z-\epsilon_k-\Delta E+\bar{\epsilon}_f)}\ . \tag{6.12}$$

Apart from the weight factor $|\,\langle 0\,|\,\tilde{0}\rangle\,|^2$ this is of the same form as in the purely electronic problem, but with the renormalizations $\epsilon_f\to\bar{\epsilon}_f$ and $\tilde{V}_k\to\bar{V}_k$, i.e., $\tilde{\Gamma}\to\bar{\Gamma}$. Around energies $z=n\omega_0$ ($n=1,2,\ldots$) the spectrum has satellite structures. To describe the nth-satellite structure the approximation (6.9) has to be replaced by

$$\tilde{\Gamma}(z-h_k)\approx\tilde{\Gamma}(\delta z-\epsilon_k-\Delta E+\bar{\epsilon}_f)\,|\,\tilde{n}\rangle\langle\tilde{n}\,|\ , \tag{6.13}$$

where $|\,\delta z\,|=|\,z+n\omega_0\,|$ is small compared to ω_0. Using similar algebra as in the "small-z" case, we obtain

$$g_f^<(-n\omega_0+\delta z)=(1-n_f)\sum_{k\le k_f}\frac{|\,\bar{V}_k\,|^2}{(\epsilon_k-\Delta E+\bar{\epsilon}_f)^2}\frac{|\,\langle n\,|\,\tilde{0}\rangle\,|^2}{\delta z-\epsilon_k-\Delta E-|\,\langle n\,|\,\tilde{n}\rangle\,|^2\tilde{\Gamma}(\delta z-\epsilon_k-\Delta E+\bar{\epsilon}_f)}\ , \tag{6.14}$$

which, apart from the different weight factor $|\,\langle n\,|\,\tilde{0}\rangle\,|^2$, has a *different "width" renormalization* in the denominator. This different factor $|\,\langle n\,|\,\tilde{n}\rangle\,|^2$ multiplying $\tilde{\Gamma}$ has the effect that the *shape* of the nth-satellite structure depends on n. In particular, the individual terms in the k sum in (6.23) have a pole contribution which is *not* exactly at $\delta z=\epsilon_k$. The effect of the renormalization factor $|\,\langle n\,|\,\tilde{n}\rangle\,|^2$ is most drastic when it *vanishes*. This happens for $n=1$ when $\beta=\lambda^2/\omega_0^2=1$. One way to see this is to use the commutation relation $[b,b^\dagger]=1$ to show that

$$b\tilde{b}^\dagger=1-\beta+(\lambda/\omega_0)(b^\dagger-\tilde{b})+b^\dagger\tilde{b}\ , \tag{6.15}$$

where $\tilde{b}^\dagger=b^\dagger+\lambda/\omega_0$ creates the excited states of the shifted oscillator (3.17). Multipyling (6.15) from the left with $\langle 0\,|$ and from the right with $|\,\tilde{0}\rangle$ leads to

$$\langle 1\,|\,\tilde{1}\rangle=(1-\beta)\langle 0\,|\,\tilde{0}\rangle\ . \tag{6.16}$$

The only broadening of the $n=1$ satellite is therefore due to $\vec{k}$ summation, which leads to an asymmetric peak shape. Figure 13 shows the exact spectrum (4.9) for $\omega_0=20$ and $B=2$. For $\beta=\frac{1}{4}$ we only show the $n=1$ satellite, which has the largest weight. The shape of the satellite peak is clearly different from the main peak as discussed above. For $\beta=1$ the two-peak structure of the main peak is lost in the $n=1$ satellite, as we found in our approximate discussion using (6.14)–(6.16). In the exact spectra we have introduced a lifetime broadening for numerical convenience. The case $B\gg\omega_0$, but ω_0 larger than the rest of the energies in the problem, is more difficult to handle. It will be partially discussed for the case when the "f level" is extremely far below the Fermi energy ("deep-level" case)

VII. "DEEP-LEVEL" CASE

In this section we discuss the limit when the bare f level ϵ_f is so deep below the Fermi energy that n_f is almost 1 and the energy gain due to the hybridization $\bar{\epsilon}_f-\Delta E$ is the smallest energy in the problem. Then the approximation (6.1) can be used to determine the ground state. The operator $H_B(0)$ in the denominator on the rhs of (6.4) can then be dropped and the equation that determines ΔE reads

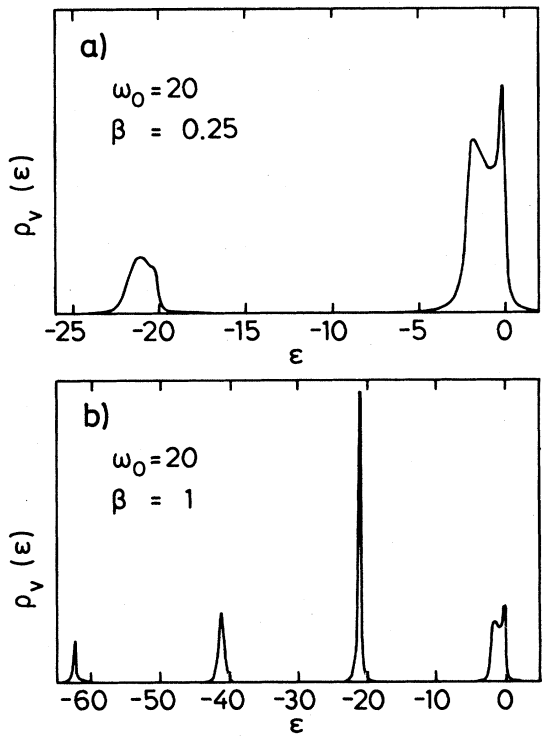

FIG. 13. Exact results for the f-level spectral function in the plasmon case. In the upper curve only the "main peak" and the first "plasmon satellite" is shown. Note the different shape of the plasmon satellite. The lower curve shows the spectrum when the width-renormalization factor $|\langle 1|\tilde{1}\rangle|^2$ for the first plasmon satellite vanishes. The parameters are $B=2$, $\tilde{\Delta}=\exp(-\beta)\tilde{\Delta}=1$, and $\bar{\epsilon}_f=-0.8$.

$$\Delta E=-\tilde{\Gamma}(\bar{\epsilon}_f-\Delta E)\ . \tag{7.1}$$

The components $|B_k\rangle$ which enter the f-level Green's function are then given by

$$|B_k\rangle=\tilde{b}_0\frac{-\tilde{V}_k}{\bar{\epsilon}_f-\Delta E-\epsilon_k}|\tilde{0}\rangle\ , \tag{7.2}$$

with

$$\tilde{b}_0^2=\left[1+\sum_{k\le k_f}\frac{|\tilde{V}_k|^2}{(\bar{\epsilon}_f-\Delta E-\epsilon_k)^2}\right]^{-1}\ . \tag{7.3}$$

Apart from the overall boson state $|\tilde{0}\rangle$, the results resemble the purely electronic problem with only the renormalization $\epsilon_f\to\bar{\epsilon}_f$. The f-level Green's function simplifies to

$$g_f^<(z)=\tilde{b}_0^2\sum_{k\le k_f}\frac{|\tilde{V}_k|^2}{(\bar{\epsilon}_f-\Delta E-\epsilon_k)^2}\times\left\langle\tilde{0}\left|\frac{1}{z-\Delta E-\epsilon_k+H_B(0)-\tilde{\Gamma}(z-h_k)}\right|\tilde{0}\right\rangle\ . \tag{7.4}$$

In the limit of an extremely deep level, the k sum in (7.4) together with the prefactor $\tilde{b}_0$ acts like a δ function and (7.4) simplifies further to

$$g_f^<(z)=\left\langle\tilde{0}\left|\frac{1}{z-\bar{\epsilon}_f+H_B(0)-\tilde{\Gamma}[z+H_B(1)]}\right|\tilde{0}\right\rangle\ , \tag{7.5}$$

where we have also used $\Delta E\approx\bar{\epsilon}_f$. Now we must distinguish the two cases $|\bar{\epsilon}_f|\gg B$ and $|\bar{\epsilon}_f|\ll B$. In the first case, the $\tilde{\Gamma}(\epsilon-i0)$ is real near $\bar{\epsilon}_f$, and small, and can therefore be neglected. One finally obtains, with $|\langle\tilde{0}|n\rangle|^2=e^{-\beta}\beta^n/n!$,

$$\rho_f(\epsilon)=e^{-\beta}\sum_{n=0}^{\infty}\frac{\beta^n}{n!}\delta(\epsilon-\bar{\epsilon}_f-n\omega_0)\ , \tag{7.6}$$

i.e., the Poisson distribution well known in core-level spectroscopy.[21] The center of gravity is at $\bar{\epsilon}_f-v\approx\epsilon_f-2n_fv$ as $n_f\approx1$. For $|\bar{\epsilon}_f|\ll B$ and a constant band density of states, $\tilde{\Gamma}(z)$ can be replaced by its constant imaginary part, $\tilde{\Delta}$, in (7.5). This leads to a Lorentzian broadening of the peaks in (7.6) and the width is given by the *unrenormalized* $\tilde{\Delta}$. This result was first discussed by Almbladh and Minnhagen.[22]

VIII. "EMPTY"-LEVEL CASE

If $\bar{\epsilon}_f$ is sufficiently high above the Fermi energy it is sufficient to use perturbation theory in the hybridization $\tilde{V}_k$. To leading order in $|\tilde{V}_k|^2$, the resolvent in (4.9) can be evaluated to zeroth order to obtain $g_f^<(z)$,

$$g_f^<(z)=\sum_{k\le k_f}|\tilde{V}_k|^2\left\langle0\left|\frac{1}{\epsilon_k-\epsilon_f-H_B(1)}[z-\epsilon_k+H_B(0)]^{-1}\times\frac{1}{\epsilon_k-\epsilon_f-H_B(1)}\right|0\right\rangle\ . \tag{8.1}$$

Inserting eigenstates of $H_B(0)$ and taking the imaginary part yields

$$\rho_f(\epsilon)=\sum_{n=0}^{\infty}\left|\left\langle 0\left|\frac{1}{\epsilon+n\omega_0-\epsilon_f-H_B(1)}\right|n\right\rangle\right|^2 \times \mathrm{Im}\tilde{\Gamma}(\epsilon+n\omega_0)/\pi \ . \tag{8.2}$$

For $\epsilon_f \gg \omega_0$ the operator $H_B(1)$ in the denominator can be neglected and (8.2) simplifies to

$$\rho_f(\epsilon)=\frac{1}{(\epsilon-\epsilon_f)^2}\mathrm{Im}\tilde{\Gamma}(\epsilon)/\pi \ , \tag{8.3}$$

exactly as in the purely electronic case, i.e, without any renormalization. For $\omega_0 \gg \epsilon_f$, again only the $n=0$ term in the sum contributes for $-\omega_0<\epsilon<0$. Inserting eigenstates of $H_B(1)$ and keeping only the leading term for large ω_0 gives

$$\rho_f(\epsilon)=\frac{1}{(\epsilon-\bar{\epsilon}_f)^2}\,|\langle 0\,|\,\tilde{0}\rangle|^2\mathrm{Im}\bar{\Gamma}(\epsilon)/\pi \ , \tag{8.4}$$

which is, again, of purely electronic form, but with renormalizations $\epsilon_f \to \bar{\epsilon}_f$ and $\tilde{\Gamma} \to |\langle 0\,|\,\tilde{0}\rangle|^2\tilde{\Gamma}$, in agreement with the discussion in Sec. VI.

IX. CONCLUSIONS

We have presented the exact solution to the model Hamiltonian (2.1) in the limit when the degeneracy N_f of the f level goes to infinity. For the corresponding model without the coupling to the boson we have also calculated corrections of order $1/N_f$ for finite N_f. Since $N_f=14$ if spin-orbit splitting is neglected, or $N_f=6$ (8) when spin-orbit splitting is included, $1/N_f$ is a small parameter and except for N_f close to unity the corrections to the $N_f \to \infty$ results are rather small. Therefore we have not discussed $1/N_f$ corrections in this paper. As shown in Sec. V the adiabatic approximation (5.6) provides a good description of the phonon case, including the transition regime near $v_c(\epsilon_f)$. There is no reason to believe that this fact has anything to do with the large-degeneracy limit discussed in this paper. For finite N_f the structure of the results, e.g., Eq. (5.24), for the spectral function, do *not* change when finite N_f values are considered. One has only to replace the purely electronic spectral function $\rho^{<}_{\epsilon_f(x)}$ in (5.24) by the corresponding result for finite N_f. Calculation of the $1/N_f$ corrections corresponding to our Hamiltonian (2.4) is therefore straightforward in the adiabatic approximation, as soon as the corrections for the purely electronic problem are known. For $N_f=1$, $\rho^{<}_{\epsilon_f(x)}$ can easily be calculated, and in the spin-fluctuation limit the main deviation from the $N_f \to \infty$ result is the absence of a Kondo peak at the Fermi energy (which has extremely small weight for $1-n_f \ll 1$ in the $N_f \to \infty$ limit). Therefore, the discussion of the spectral function in the strong-coupling mixed-valence limit given for $N_f \to \infty$, Eq. (5.39), also properly describes the $N_f=1$ case.

Earlier, we applied the theory without the phonon coupling to various cerium compounds and obtained estimates for n_f and Δ from comparison with experiments.[5–7] To apply the theory including the phonon mode one needs values for the phonon frequency ω_0 and the electron-phonon–coupling strength v. Sherrington and von Molnar[10] gave estimates for the parameters corresponding to SmS. They estimate[23] $v \approx 0.1$, $\Delta \approx 0.01$ eV, and $\beta=v/\omega_0 \approx 4$. If multiplied with the degeneracy factor N_f, the more relevant width[14] $\tilde{\Delta}=N_f\Delta$ is comparable to v, which may bring us into the strong-coupling mixed-valence regime, and the criterion for the applicability of the adiabatic approximation ($\beta \gg 1$) is almost reached.

For Ce compounds, we have deduced much larger values of Δ, typically $\Delta \sim 0.1$ eV. Multiplied with the degeneracy factor, this leads to values of $\tilde{\Delta}$ which should be larger than v. We are therefore then in the weak-coupling mixed-valence regime which is properly described by the mean-field approximation (5.24). To a good approximation the theory *with* coupling to the phonon therefore leads to the *same* spectrum, f occupancy, magnetic susceptibility, etc. as the theory *without* the coupling, if the *bare-f*-level position is renormalized by $-2n_fv$ in the latter case. The results presented in this paper, therefore, do not alter the conclusion we have drawn from our calculations without the phonon coupling in Refs. 5 and 6.

Our results clearly show that the question of the renormalization of the coupling $\tilde{\Delta}$ due to polaronic effects generally depends on the experimental question one asks. In the "phonon" case the renormalization "appearing" in the ground state is absent in the photoemission spectrum. In the "plasmon" case the renormalization can differ from satellite to satellite.

APPENDIX A

In this appendix we present some of the details of the calculations in the limit $B \to 0$. In this case the function $\tilde{\Gamma}(z)$ [Eq. (3.15)] takes the form

$$\tilde{\Gamma}(z)=\tilde{V}^2/z \ . \tag{A1}$$

The pole of $\tilde{\Gamma}(z)$ is at $z=0$ because we have chosen $\epsilon_F=0$. Concerning the *ground-state calculation* (3.14), the $N_f=\infty$ and $B=0$ limits of the Hamiltonian (2.1) are isomorphic to the nondegenerate ($N_f=1$) limit of (2.1), where the metal band is replaced by a single level $|\,b\,\rangle$ with energy $\epsilon_b=0$ and the system has a *single* electron. The single-electron case of the model (2.1) for $N_f=1$ was studied in detail by Hewson and Newns.[12] The exact ground-state calculation is not appreciably simplified by the special choice (A1), but the approximate adiabatic phonon treatment presented in Sec. V can be performed rather easily. The equation for the adiabatic electron ground-state energy, (5.10), reduces to a quadratic equation with the solution

$$\Delta E(\epsilon_f(x))=\frac{\epsilon_f(x)}{2}-\left[\left[\frac{\epsilon_f(x)}{2}\right]^2+\tilde{V}^2\right]^{1/2} , \tag{A2}$$

with $\epsilon_f(x)=\epsilon_f+\lambda x$. Differentiating with respect to ϵ_f yields $n_f(\epsilon_f(x))$,

$$n_f(\epsilon_f(x))=\frac{1}{2}\left[1-\frac{\epsilon_f(x)/2}{\{[\epsilon_f(x)/2]^2+\tilde{V}^2\}^{1/2}}\right]. \quad \text{(A3)}$$

Since $n_f(\epsilon_f)-\frac{1}{2}$ is an odd function of ϵ_f, the inflection point is at $\epsilon_f=0$ and the maximum of the negative slope is $-n_f'(0)=\frac{1}{4}|\tilde{V}|$. According to (5.15) or (5.29), this leads to the critical value

$$v_{\rm crit}=2|\tilde{V}|\ . \quad \text{(A4)}$$

The ϵ_f value of the critical point follows from (5.15) as

$$(\epsilon_f)_{\rm crit}=v_{\rm crit}\ . \quad \text{(A5)}$$

From the fact that $n_f(\epsilon_f)-\frac{1}{2}$ is an odd function with respect to ϵ_f, it also follows that the critical line $v_c(\epsilon_f)$ in the (ϵ_f,v) plane, where the first-order transition occurs in the limit $\omega_0\to 0$, is the straight line $v=\epsilon_f$. To see this we consider an $\epsilon_f>(\epsilon_f)_{\rm crit}$ and increase v from $v_{\rm crit}$ until in solving (5.15) we come to the value $v_c(\epsilon_f)$ where the three solutions are such that the Maxwell criterion of equal areas is fulfilled. If we denote the n value which for this value of v corresponds to the maximum of $V_0(x)$ by $n_{\max}(\epsilon_f)$ and the corresponding value of u by $u_{\max}(\epsilon_f)$, Eq. (5.15) reads

$$n_{\max}(\epsilon_f)=-\frac{1}{2v_c(\epsilon_f)}[u_{\max}(\epsilon_f)-\epsilon_f]\ . \quad \text{(A6)}$$

For n_f given by (A3), $n_{\max}(\epsilon_f)=\frac{1}{2}$ and $u_{\max}(\epsilon_f)=0$ for all values of $\epsilon_f>(\epsilon_f)_{\rm crit}$ and therefore we obtain, for $\epsilon_f>(\epsilon_f)_{\rm crit}$,

$$v_c(\epsilon_f)=\epsilon_f\ . \quad \text{(A7)}$$

The equivalence of the $N_f=\infty$ and the ($N_f=1$, one-electron) case which holds for the ground-state calculation does *not* hold for the spectral function $\rho_f(\epsilon)$ because, for the one-electron (and $N_f=1$) system, the removal of that one electron makes the electronic problem in the final state trivial (no electron), while for the $N_f=\infty$ case the removal of one electron does not change the character of the relevant electronic states. The expression for the spectral function $\rho^<_{\epsilon_f(x)}$ in (5.30) simplifies using (A1) to

$$\rho^<_{\epsilon_f(x)}(\epsilon)=n_f(\epsilon_f(x))\left[[1-n_f(\epsilon_f(x))]\delta(\epsilon)+n_f(\epsilon_f(x))\delta\left\{\epsilon+2\left[\left[\frac{\epsilon_f(x)}{2}\right]^2+\tilde{V}^2\right]^{1/2}\right\}\right]. \quad \text{(A8)}$$

To obtain the approximate spectrum, $\tilde{\rho}(\epsilon)$, this expression has to be used on the rhs of (5.23). One of the two peaks in $\rho^<_{\epsilon_f(x)}(\epsilon)$ is independent of x. This is the peak at threshold $\epsilon=0$. Therefore only the other peak obtains a phonon broadening of order $(v\omega_0)^{1/2}$, as described in (5.25)–(5.28). This is confirmed by comparisoon with the exact calculation as shown in Fig. 9. To resolve the phonon structure of the broadened peak in the exact calculation, we would have to choose a lifetime broadening y which is smaller than ω_0. An approximate description of that fine structure could be easily obtained (for the limit $B=0$ discussed here) by also treating the $(N-1)$-electron final states in the adiabatic approximation using (5.32).

APPENDIX B

In all of the exact numerical calculations that we have performed for a finite bandwidth B, we have used a half-filled band with a semielliptical density of states. In this appendix we discuss the case of a constant band density of states, especially in the limit $B\to\infty$. The corresponding function $\tilde{\Gamma}(z)$ [Eq. (3.15)] is given by

$$\tilde{\Gamma}(z)=(\tilde{\Delta}/\pi)\ln[z/(B+z)]\ . \quad \text{(B1)}$$

In the limit $B\to\infty$ we can drop the z in the denominator of the logarithm in (B1) for all relevant energies z. The equation for the ground state, (3.14), can then be written as

$$\{H_B(0)+(\tilde{\Delta}/\pi)\ln[\pi(\epsilon_f^*-\Delta E^*+H_B(1))/\tilde{\Delta}]-\Delta E^*\}\,|B_0\rangle=0\ , \quad \text{(B2)}$$

with

$$\epsilon_f^*=\epsilon_f+(\tilde{\Delta}/\pi)\ln(\pi B/\tilde{\Delta}) \quad \text{(B3)}$$

and

$$\Delta E^*=\Delta E+(\tilde{\Delta}/\pi)\ln(\pi B/\tilde{\Delta})\ .$$

This scaling behavior has been discussed by various authors[20] for the $\lambda=0$ limit of the model (2.1). As in the zero-bandwidth case, the special choice (B1) for $\tilde{\Gamma}(z)$ does not simplify the exact ground-state calculation. In the adiabatic approximation, however, it is again possible to obtain some analytical results. If we introduce the "Kondo temperature" $\delta:=\epsilon_f^*-\Delta E^*$ the equation for the adiabatic ground-state energy (5.10) reads

$$\delta(\epsilon_f(x))=\epsilon_f(x)-(\tilde{\Delta}/\pi)\ln[\delta(\epsilon_f(x))\pi/\tilde{\Delta}]\ , \quad \text{(B4)}$$

with $\epsilon_f(x)=\epsilon_f^*+\lambda x$. The adiabatic f occupancy is given by

$$n_f(\epsilon_f(x))=\frac{\tilde{\Delta}/\pi}{\delta(\epsilon_f(x))+\tilde{\Delta}/\pi}\ . \quad \text{(B5)}$$

If we insert (B5) in (B4) we can obtain $\epsilon_f(x)$ as a function of $n_f(\epsilon_f(x))$,

$$\epsilon_f(x)=\frac{\tilde{\Delta}}{\pi}\left[\frac{1-n_f(\epsilon_f(x))}{n_f(\epsilon_f(x))}+\ln\frac{1-n_f(\epsilon_f(x))}{n_f(\epsilon_f(x))}\right], \quad \text{(B6)}$$

which allows us to plot $\epsilon_f(x)$ as a function of $n_f(\epsilon_f(x))$. The plot of Fig. 1 shows that, contrary to the $B=0$ limit, $n_f(\epsilon_f)$ has no symmetry behavior around its inflection point. Using (B4) and (B6) one can show that

$$\frac{dn_f}{d\epsilon_f}=-\frac{\tilde{\Delta}\delta/\pi}{(\delta+\tilde{\Delta}/\pi)^3}=-(\pi/\tilde{\Delta})(1-n_f)n_f^2 \quad \text{(B7)}$$

and

$$\frac{d^2 n_f}{d\epsilon_f^2} = (2\delta - \tilde{\Delta}/\pi)\frac{\tilde{\Delta}\delta/\pi}{(\delta+\tilde{\Delta}/\pi)^5} . \tag{B8}$$

The inflection point, which determines the critical point $(v_{\rm crit}, (\epsilon_f^*)_{\rm crit})$, therefore occurs for $\delta = \tilde{\Delta}/2\pi$, i.e, for $n_f = \frac{2}{3}$. Using (B7) to obtain the slope, we find

$$v_{\rm crit} = \tfrac{27}{8}(\tilde{\Delta}/\pi) \approx 1.07\tilde{\Delta} , \tag{B9}$$

and from (5.15),

$$(\epsilon_f^*)_{\rm crit} = \tfrac{4}{3} v_{\rm crit} + \epsilon_f^*(\tfrac{2}{3}) , \tag{B10}$$

where

$$\epsilon_f^*(\tfrac{2}{3}) = (\tilde{\Delta}/\pi)(0.5 - \ln 2) \approx -0.198\tilde{\Delta}/\pi$$

is the ϵ_f^* value corresponding to $n_f = \frac{2}{3}$. The critical line $v_c(\epsilon_f^*)$ which starts at the critical point is, according to (6), given by

$$v_c(\epsilon_f^*) = \frac{\epsilon_f^* - u_{\rm max}(\epsilon_f^*)}{2n_{\rm max}(\epsilon_f^*)} . \tag{B11}$$

As we have no symmetry around the inflection point this is only a straight line asymptotically for large ϵ_f^*. The expression (5.30) for the spectral function $\rho^{<}_{\epsilon_f(x)}(\epsilon)$ does not simplify very much compared to the general case, so we do not consider it any further in this appendix.

[1]See, e.g., J. M. Lawrence, P. S. Riseborough, and R. D. Parks, Rep. Prog. Phys. **41**, 1 (1981), for a review and further references.

[2]*Valence Fluctuations in Solids,* edited by L. M. Falicov, W. Hanke, and M. P. Maple (North-Holland, Amsterdam, 1981).

[3]P. W. Anderson, Phys. Rev. **124**, 41 (1961).

[4]T. V. Ramakrisnan, in *Valence Fluctuations in Solids,* Ref. 2, p. 13; T. V. Ramakrishnan and K. Sur, Phys. Rev. B **26**, 1798 (1982); P. W. Anderson, in *Valence Fluctuations in Solids,* Ref. 2, p. 451.

[5]O. Gunnarsson and K. Schönhammer, Phys. Rev. Lett. **50**, 604 (1983).

[6]O. Gunnarsson and K. Schönhammer, Phys. Rev. B **28**, 4315 (1983).

[7]J. C. Fuggle, F. U. Hillebrecht, J.-M. Esteva, R. C. Karnata, O. Gunnarsson, and K. Schönhammer, Phys. Rev. B **27**, 4637 (1983); J. C. Fuggle, F. U. Hillebrecht, Z. Zolnierek, R. Lässer, Ch. Freiburg, O. Gunnarsson, and K. Schönhammer, Phys. Rev. B **27**, 7330 (1983); F. U. Hillebrecht, J. C. Fuggle, G. A. Sawatzky, M. Campagna, O. Gunnarsson, and K. Schönhammer (unpublished); O. Gunnarsson, K. Schönhammer, J. C. Fuggle, F. U. Hillebrecht, J.-M. Esteva, R. S. Karnatac, and B. Hillebrand, Phys. Rev. B **28**, 7330 (1984).

[8]N. Read and D. M. Newns, J. Phys. C **16**, 3273 (1983); P. Coleman Phys. Rev. B **29**, 3035 (1984); Y. Kuramoto Z. Phys. B **53**, 37 (1983); J. W. Rasul and A. C. Hewson, J. Phys. C **16**, L933 (1983); C **17**, 2555 (1984); F. C. Zhang and T. K. Lee, Phys. Rev. B **28**, 33 (1983).

[9]P. Schlottmann, Phys. Rev. Lett. **50**, 1697 (1983); Z. Phys. B **52**, 127 (1983); E. Ogievetski, A. M. Tsvelick, and P. B. Wiegmann, J. Phys. C **16**, L797 (1983).

[10]D. Sherrington and S. von Molnar, Solid State Commun. **16**, 1347 (1975).

[11]F. D. M. Haldane, Phys. Rev. B **15**, 281 (1977).

[12]A. C. Hewson and D. M. Newns, J. Phys. C **12**, 1665 (1979).

[13]A. C. Hewson and D. M. Newns, J. Phys. C **13**, 4477 (1980).

[14]W. Kohn, T. K. Lee, and Y. R. Lin-Liu, Phys. Rev B **25**, 3557 (1982).

[15]A. C. Hewson and D. M. Newns, Jpn. Appl. Phys. Suppl. **2**, 121 (1974).

[16]K. Sinjo, S. Sugano, and T. Sasada (unpublished); K. Sinjo and S. Sugano (unpublished).

[17]O. M. Braun and A. I. Volotkin, Surf. Sci. **131**, 148 (1983).

[18]W. Domcke and L. S. Cederbaum, Phys. Rev. A **16**, 1465 (1977); J. Phys. B **13**, 2829 (1980).

[19]M. Born and K. Huang, *Dynamical Theory of Crystal Lattices* (Oxford University Press, London, 1954).

[20]See e.g., F. D. M. Haldane, in *Valence Fluctuations in Solids,* Ref. 2, p 153.

[21]D. Langreth, Phys. Rev. B **1**, 471 (1970).

[22]C. O. Almbladh and P. Minnhagen, Phys. Rev. B **17**, 929 (1977).

[23]We have connected the estimates for v in Ref. 10 by a factor of $\frac{1}{4}$, due to an apparent mistake in the ionic radii of Sm.